MARCELL JOSÉ DE ANDRADE OLIVIER

EXPERIMENTAL STUDY OF RIBBED SANDWICH PANELS UNDER AXIAL COMPRESSION

Dissertation submitted to the Program in Civil Engineering of the Universidade Federal de Viçosa in partial fulfillment of the requirements for the degree of *Magister Scientiae*.

Adviser: José Maria Franco de Carvalho

Co-advisers: Carol Ferreira Rezende Santos
Gustavo de Souza Veríssimo

VIÇOSA – MINAS GERAIS
2022

Ficha catalográfica elaborada pela Biblioteca Central da Universidade Federal de Viçosa - Campus Viçosa

T

O49e 2022

Olivier, Marcell José de Andrade, 1996-

Experimental analysis of ribbed sandwich panels under axial compression / Marcell José de Andrade Olivier. – Viçosa, MG, 2022.

1 dissertação eletrônica (79 f.): il. (algumas color.).

Texto em inglês.

Orientador: José Maria Franco de Carvalho.

Dissertação (mestrado) - Universidade Federal de Viçosa, Departamento de Engenharia Civil, 2022.

Referências bibliográficas: f. 72-79.

DOI: https://doi.org/10.47328/ufvbbt.2023.021

Modo de acesso: World Wide Web.

1. Sanduíche (Construção). 2. Resistência de materiais. I. Carvalho, José Maria Franco de, 1979-. II. Universidade Federal de Viçosa. Departamento de Engenharia Civil. Programa de Pós-Graduação em Engenharia Civil. III. Título.

CDD 22. ed. 693.92

Bibliotecário(a) responsável: Euzébio Luiz Pinto CRB-6/3317

MARCELL JOSÉ DE ANDRADE OLIVIER

EXPERIMENTAL STUDY OF RIBBED SANDWICH PANELS UNDER AXIAL COMPRESSION

Dissertation submitted to the Program in Civil Engineering of the Universidade Federal de Viçosa in partial fulfillment of the requirements for the degree of *Magister Scientiae*.

APPROVED: December 02, 2022.

Assent:

Documento assinado digitalmente
gov.br
MARCELL JOSE DE ANDRADE OLIVIER
Data: 02/02/2023 17:19:24-0300
Verifique em https://verificador.iti.br

Marcell José de Andrade Olivier
Author

Documento assinado digitalmente
gov.br
JOSE MARIA FRANCO DE CARVALHO
Data: 02/02/2023 18:52:16-0300
Verifique em https://verificador.iti.br

José Maria Franco de Carvalho
Advisor

ACKNOWLEGMENT

Um desafio equiparável ao de concluir o Mestrado e escrever esta Dissertação, foi o de colocarem palavras esse sentimento de gratidão a todos os que me ajudaram a finalizar esta importanteetapa da minha vida. Foi sem dúvida uma viagem repleta de emoções fortes até o fim.

Agradeço primeiramente a Deus pela vida, pela saúde e por me permitir concluir esse trabalho.

Aos meus familiares, em especial aos meus pais, Valéria e José Geraldo, pelo apoio incondicional em toda minha vida e à minha tia Licia por todo suporte em Viçosa.

Aos professores José Maria Franco de Carvalho e Carol Ferreira Rezende Santos na elaboraçãodo tema e auxilio na elaboração desta dissertação.

Aos professores José Luiz Rangel Paes e Gustavo de Souza Verissimo, pela colaboração na realização do ensaio experimental e na análise dos dados obtidos em laboratório.

Além disso, por todos os ensinamentos não apenas técnicos, mas também de vida, que me fizeram crescer como pessoa e com certeza vou levar por toda vida.

Ao professor Humberto Varum pela participação na banca.

Aos colegas do mestrado, pelas contribuições e trocas de conhecimentos ao longo do processo.

Aos demais professores e funcionários do DEC, em especial ao técnico do laboratório de estruturas Robson por todo auxílio e ensinamentos durante a preparação dos ensaios.

À CAPES (o presente trabalho foi realizado com apoio da Coordenação de Aperfeiçoamento de Pessoal de Nível Superior – Brasil (CAPES) – Código de Financiamento 001).

ABSTRACT

OLIVIER, Marcell José de Andrade, M.Sc., Universidade Federal de Viçosa, December 2022. **Experimental study of ribbed sandwich panels under axial compression**. Advisor: José Maria Franco de Carvalho. Co-advisors: Carol Ferreira Rezende Santos and Gustavo de SouzaVeríssimo.

The idea of a construction model that can add sustainability, lightness, significant stiffness, and strength to the precast industry has contributed to the advancement in research on sandwich panels. These panels are manufactured and improved to obtain a high strength-to-weight ratio, stiffness-to-weight ratio, and other construction advantages such as fast assembly, cost reduction, and good insulation properties. This dissertation presents an axial compression analysis of sandwich panels with self-compacting concrete, EPS, and reinforcement to offer tothose interested in alternative construction methods information on a viable solution advantageous at various levels that can be adapted and equally suited to their construction needs. This work presents a summary of the various applications, followed by a review that describes the influence of each component of the panel in its structural capacity. The advantages and disadvantages of the panels are addressed, accompanied by several studies performed applying alternative materials and geometries. A laboratory study was conducted with six prototypes, where the influence of slenderness, materials used, and geometry on the failure mode to axial compression was evaluated. Finally, a brief conclusion of what was covered throughout the dissertation is presented.

Keywords: Sandwich panel. Experimental analysis. Precast concrete element. Axial compression. Constructive system.

RESUMO

OLIVIER, Marcell José de Andrade, M.Sc., Universidade Federal de Viçosa, dezembro de 2022. **Estudo experimental de painéis sanduíche nervurados sob compressão axial**. Orientador: José Maria Franco de Carvalho. Coorientadores: Carol Ferreira Rezende Santos e Gustavo de Souza Veríssimo.

A ideia de um modelo construtivo que possa agregar sustentabilidade, leveza, significativa rigidez e resistência na indústria do pré-moldado contribuiu para o avanço em pesquisas voltadas para painéis sanduíche. Estes painéis são aperfeiçoados e fabricados com o objetivo de obter elevada relação resistência/peso próprio, rigidez/peso próprio e outras vantagens a nível construtivo como a montagem rápida, a redução de custos e boas propriedades de isolamento. Nesta dissertação é apresentada uma análise a compressão axial de painéis sanduíche com concreto autoadensável, EPS e armadura, com o intuito oferecer aos interessados em métodos construtivos alternativos informações sobre uma solução viável, vantajosa a vários níveis e que pode ser adaptada e igualmente adequada às suas necessidades construtivas. Este trabalho apresenta um resumo das diversas aplicações, seguindo de uma revisão que descreve a influência de cada componente do painel em sua capacidade estrutural. As vantagens e desvantagens dos painéis são abordadas, acompanhados de vários estudos realizados aplicando materiais e geometrias alternativas. Foi realizado um estudo em laboratório com 6 protótipos, onde se avaliou a influência da esbeltez, dos materiais utilizados e da geometria no modo de falha a compressão axial. Por fim, é apresentada uma conclusão sucinta do que foi abordado durante toda a dissertação.

Palavras-chave: Painel sanduíche. Elemento pré-fabricado de concreto. Compressão axial. Sistema construtivo.

TABLE OF CONTENTS

CHAPTER 1. General introduction

1.1 Introduction

Sandwich structures have high versatility in their properties, depending on the several combinations of coatings and core configurations. The advantages offered by sandwich structures include a high stiffness/weight and strength/weight ratio, excellent shock resistance,good damping properties, good thermal and acoustic properties, the possibility of combining different properties and functions within a single construction, in addition to the reduction in time and costs in the production of buildings (CORE, 2013; KUJALA; KLANAC, 2005).

The sandwich structures market has been expanding its application every year, from the production of satellites to large aircraft. Several countries use composite sandwich constructions for the hulls of their navy ships. Another application is wind energy systems. Due to the growing need for alternative energy sources, mill systems are developed based on composite sandwich structures (VINSON, 2005).

The idea behind the sandwich panels is to increase the bending inertia/weight ratio (GAY; HOA, 2007). Many materials and geometric combinations are possible today, both for the coreand the wythes (NEVEU; CASTANIÉ; OLIVIER, 2019). However, for aeronautical applications, these combinations are reduced. The main materials used in the cores are honeycomb geometries based on Nomex, aluminum alloy or a limited number of high-quality foams. Likewise, one will find mainly aluminum alloys and laminates based on fiberglass, carbon or Kevlar for wythes. (TOMBLIN *et al.*, 1999).

Sandwich structures are increasingly gaining ground in civil construction. Typical sandwich panels used in structural applications consist of two thin, rigid, high-strength wythes held together by a thick, relatively flexible core. The wythes provide most of the flexural stiffness for the panel. The core, in line with the shear connectors, provides the shear stiffness and composite interaction between the wythes. Due to its thickness between the wythes, the core is responsiblefor increasing the bending inertia of the set. (ABBADI *et al.*, 2006; DAWOOD *et al.*, 2010; MAMALIS *et al.*, 2008). In addition to the wythes and the core, connectors arranged along the thickness of the panel are used to promote interaction between the wythes. Thus, whilethe wythes, together with the core, are responsible for promoting the flexural stiffness of the set, the shear connectors contribute to the shear stiffness, promoting the

composite behavior. The sandwich structure efficiently uses the unique characteristics of different materials.

Over the years, several studies on the structural, thermal and acoustic performance of sandwichpanels were conducted. In the structural context, the studies evaluate the influence of the materials of the core and wythes, shear connector and the geometric configuration, and thematerials on the ultimate capacity and failure mode of the panels.

1.2 General information about sandwich panels

The sandwich panels used in civil construction can have a structural or non-structural function. Non-structural sandwich panels are commonly used as partitions, and ceilings, while non- structural sandwich panels are used as floor and wall elements. The difference betweenstructural and non-structural panels is their bearing capacity. It is common to use reinforced orprestressed concrete on the wythes in structural panels, while in non-structural panels, materials of lower mechanical strength are used (O'HEGARTY; KINNANE, 2020).

According to Jones (1975), Mendonça (2005) and Tita (2007), different failure modes are exhibited by sandwich panels. The most common modes are wythe yielding or failure, connectorshear, global and local panel buckling, wythe warping, and core crushing. When used as structuralpanels in wall systems, the panels are subjected to compression, in which the predominant failure modes consist of crushing the concrete wythes or global or local buckling of the panels.(JONES, 1975; MENDONÇA, 2005; TITA, 2007)

Failure by compression in sandwich panels is related to the overall slenderness of the wall. Forheight/thickness up to 24, there is a more significant crushing tendency at the top, while for panels with slenderness greater than 24, deformations caused by buckling closer to the middle are observed. (DANIEL RONALD JOSEPH; PRABAKAR; ALAGUSUNDARAMOORTHY, 2018; MUGAHED AMRAN *et al.*, 2019)

Lightweight expanded polyurethane foams are commonly used as the core material of sandwichpanels. In general, these do not contribute to the compressive strength of the panels, with the only objective of guaranteeing the spacing between the concrete wythes. Studies such as those of CoDyre & Fam (2016) evaluated the influence of the density of Polyisocyanurate (PIR) foams on the compressive strength of sandwich panels. Three density

levels (32 kg/m³, 64 kg/m³ and 96 kg/m³) were evaluated. The results showed an increase in the ultimate capacity of the panel when subjected to compression. For densities of 64 and 96 kg/m³, the final capacity increased by around 71% and 170%, respectively.(CODYRE; FAM, 2016)

Another fundamental component in sandwich structures is the shear connectors, which connectthe two concrete wythes and produce a composite sandwich behavior. Different typologies and materials used in the connectors were evaluated over the years. For example, Chen et al. (2015)produced fiberglass connectors with three different shapes. The mechanical performance of thepanels was evaluated through four-point and three-point bending tests. They observed that panels with continuous connectors showed higher strength when compared to those with discontinuous connectors. The connectors proposed by the authors caused a ductile behavior inall their configurations. In addition, prototypes with continuous connectors obtained flexural strength close to solid panels, with a slight loss of strength, but showing weight and cost reduction (CHEN *et al.*, 2015).

Given the scarcity of information on the axial compression performance of sandwich panels, this work reviews the main compression failure modes in such structures, proposes and evaluates a sandwich panel typology with longitudinal and transverse ribs in order to improve the compressive behavior while maintaining low self-weight and satisfactory mechanical performance, allowing the optimization of the compressive strength/weight ratio when compared to the sandwich panels proposed in the literature.

1.3 Objectives

The main objective of this work is to produce and assess the structural performance of a sandwich panel composed of small thicknesses concrete wythes, EPS core and concrete bridge connectors (ribs) submitted to axial compression loads. For this, the following specific objectives were defined:

- To propose, design and produce prototypes of sandwich panels with different heights and configurations for the concrete bridge connectors (ribs).
- To evaluate the influence of global slenderness, geometry and ultimate capacity parameters on axial compression regarding the failure modes observed during the test.

- To gather and evaluate equations found in the literature regarding their ability to accurately predict the axial compression behavior observed in laboratory tests.

1.4 Outline

This dissertation is organized into four chapters. The first briefly introduces the theme, presenting a general framework, objectives, and scientific contributions.

In the second chapter, a bibliographic review describes the panels and each component's influence on the system's mechanical properties. After these theoretical descriptions, a comparison between studies is carried out with a focus on axial compression since it is little discussed compared to other mechanical analyses but has a significant influence when panels are used as load-bearing walls. A description of the equations proposed by several authors is also made, presenting the results of the parameters that, according to them, have the most significant influence on performance under axial compression.

The third chapter brings a laboratory study carried out in a typology of sandwich panels proposed, evaluating the ultimate capacity of axial compression and the influence of the components on the failure mode of prototypes with heights up to 2 meters. In addition, equations of the literature are evaluated regarding the application of this model, thus verifying which one was more accurate in predicting the experimental results.

In the fourth and last chapter, the final considerations are presented, where the main conclusionsof the work are mentioned, and possible future developments are suggested.

CHAPTER 2. Sandwich panels – a review of new technologies, testing and design regarding load-bearing capacity

Abstract

Since the 1930s, sandwich panels have evolved, highlighting the precast concrete variant largely applied in construction today. New technologies in materials, insulating cores and shearconnectors have been investigated in order to reduce the weight and improve structural performance. The commonly adopted solution consists of reducing the thickness of the concretewythes and using a low-density core; however, reducing the thickness increases both theslenderness of the wythes and the whole panels, causing concern and making them more susceptible to local and global buckling failure. Recent research has addressed the load-carrying capacity of sandwich panels subjected to compression tests and the influence of their components on a set of configurations, including different shear connectors, core materials, and geometries. Therefore, a review aimed at analyzing the compressive behavior of sandwich panels is opportune. This chapter reviews the main compression failure modes in sandwich panels, discussing the influence of each structural sandwich component (wythes, core, connectors). In addition, considerations on new materials, technologies and prediction equations for structural design are also presented.

2.1 Introduction

Structural insulated panels (SIPs) have been largely used as part of buildings, specifically walls, roofs and floors in concrete and steel structures (SMITH, 2011). The first reports on the production of sandwich panels date back to the 1930s. Originally, SIPs were composed of a rigid foam core with plywood sheet wythes (MUGAHED AMRAN *et al.*, 2020; PANJEHPOUR; ALI; VOO, 2013). Different typologies were proposed between 1930 and 1950, but none presented adequate quality. In the 1990s, the precast concrete sandwich panel (PCSP) typology was proposed and patented by Tadros et al. (1995), becoming the best-known SIP typology (TADROS, M. K., SALMON, D. C., EINEA, A., AND CULP, 1995).

A PCSP comprises two layers of concrete sandwiched with a lightweight foam core inthe middle. The layers are connected using steel shear connectors (ALCHAAR; ABED, 2020; ATOYEBI OLUMOYEWA *et al.*, 2018), concrete "bridges" (PESSIKI; MLYNARCZYK, 2003; SEEBER *et al.*, 1997), reinforced polymer fiberglass (GFRP) (FLANSBJER *et al.*, 2018; LEE *et al.*, 2018) or carbon fiber reinforced polymer (CFRP) (KIM; YOU, 2015).

Recent reviews address innovations in thermal analysis methods, flexural response, design innovations, new materials and shapes for cores and shear connectors, use of nanotubes, main problems in sandwich structure designs, numerical analysis methods, fire performance, environmental impact, application of sandwich structure in the naval industry, and damage analysis using ultrasound techniques.

The mechanical performance of sandwich panels should be experimentally, analytically and numerically investigated to obtain a better agreement between the predicted and real behavior of the panels. Due to the innovative nature of this element, its behavior is not yet fully known; therefore, experimental tests are almost always necessary to evaluate the structural behavior and failure modes of precast concrete panels. Bending tests are commonly used to evaluate thepanel performance for loads (AAMIR MAZHAR *et al.*, 2021; CUI *et al.*, 2021) acting perpendicular to the concrete wythes (wind, dead or live loads). Bending tests are also used to evaluate the shear behavior and connection between the concrete wythes. As it is a sandwich structure, the shear connectors are essential to maintain the connection between the wythes; therefore, the diagonal compression test is also frequently used to evaluate such behavior (AHMAD; SINGH, 2021; SERPILLI; CLEMENTI; LENCI, 2021). Compression

tests (BENAYOUNE *et al.*, 2007;DANIEL RONALD JOSEPH; PRABAKAR; ALAGUSUNDARAMOORTHY, 2018; GARA *et al.*, 2012; MUGAHED AMRAN *et al.*, 2016) are used to evaluate theinfluence of different parameters on the load-bearing capacity and failure mode.

However, references to the compressive behavior of sandwich panels are scarce in the literatureand have not been adequately addressed in recent reviews. This article, therefore, aims to present a review of the main failure modes due to compression in sandwich panels, discussing the influence of each component of the structural sandwich (wythes, core, connectors). In addition, considerations on new materials, technologies and prediction equations for structuraldesign are also presented.

2.2 Structural behavior

In the last decade, researchers have investigated the influence of different parameters on the ultimate capacity of the panels, among them the global slenderness, thickness of the concrete walls, the material of the wythes and core, type of connector (CARBONARI et al., 2013; O'HEGARTY et al., 2019; SHAMS et al., 2014; MUGAHED AMRAN et al., 2019). The
parameters are generally investigated from experimental bending and compression tests, in which the choice between the type of test depends on the variable investigated. Flexural tests are widely used in evaluating the efficiency of the connectors in developing the degree of connection of the concrete wythes. In contrast, compression tests are widely used in evaluating parameters such as the slenderness of the panel and concrete wythes, among others.

In addition to experimental studies, numerical studies have also been conducted to obtain moreinformation about the parameters that govern the ultimate capacity of the panels to promote reliable results for the proposition of analytical models.

2.3 Behavior under compressive load

Compression tests are commonly used in evaluating the influence of global slenderness, local slenderness of the wythes, component materials and the typology of connectors used in the

connection of the wythes, in the ultimate capacity and failure mode of the panels.

The tests can be carried out on full-scale specimens or small specimens (specimens with reduced height), with centered or eccentric loading, with or without lateral loads. Due to the ease of testing and accuracy of results, compression tests are commonly conducted on full-scale prototypes with centered loading and no lateral loads. Concrete wall design standards recommend that the evaluation of the ultimate capacity of concrete walls must be conducted assuming a small eccentricity; however, experimental studies involving the application of eccentric loads in structural panels are scarce in the literature, which can be attributed to the difficulty of assembling the test.

Figure 2.1 – (a) Top-end rotation failure (JOSEPH et al., 2018); (b) - Top-end rotation failure(MUGAHED AMRAN et al., 2019); (c) - buckling with wythe detachment (CUI et al., 2021).

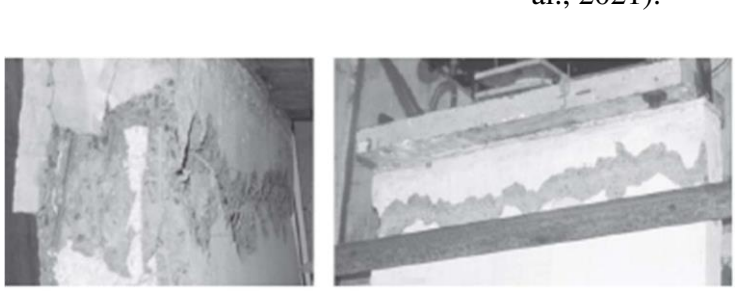

(a)

(b)

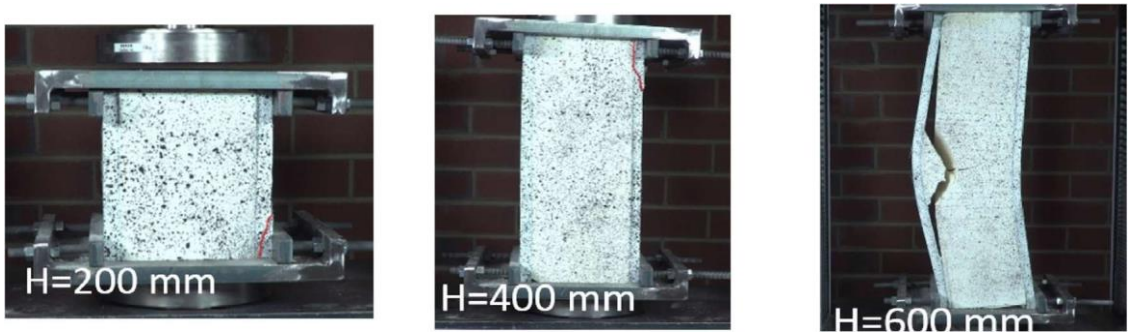

(c)

Compression failure is closely linked to the overall slenderness of the panels. For slenderness (height/thickness) of up to 24, it is noticed a more significant buckling tendency in the upper end, while for panels with slenderness greater than 24, buckling deflections are observed closerto the mid-height (JOSEPH; PRABAKAR; ALAGUSUNDARAMOORTHY, 2018; AMRAN *et al.*, 2019) (Figure 2.1). Studies conducted by Joseph et al. (2018) in sandwich panels with global slenderness equal to 20 show the need of inserting a concrete beam at the prototype's top and bottom ends in order to avoid premature collapse by stress concentration.

The authors also realized that the compression panel's performance is strongly impacted by the presence of shearconnectors, which the absence can result in the detachment of the concrete wythes, reducing the structural capacity of the panels (CUI *et al.*, 2021) (Figures 2.1).

2.3.1 Concrete wythes (wythes)

2.3.1.1 Thickness

Recent research has sought to develop new panels with thicknesses of less than 300 mm in order to optimize the dimension and reduce the weight of the panels (CARBONARI *et al.*, 2013; O'HEGARTY *et al.*, 2019; SHAMS, HORSTMANN and HEGGER, 2014). However, reducing the thickness and apparent specific weight proves to be a great challenge, as the structural properties cannot be compromised.

Since the sandwich panels are basically composed of concrete wythes and a lightweight material core interconnected by shear connectors, reducing the thickness of the concrete sheet wythes can compromise the structural stability. To evaluate the influence of concrete wall thickness on the ultimate capacity of panels submitted to axial compression, Amran et al. (2019) evaluated seven experimental models with thicknesses ranging from 105 mm to 225 mm, keeping the same height of 3000 mm for all the specimens (Figure 2.2). The authors confirmed that reducing the thickness of the panel resulted in a more significant displacement in the central portion of the prototype, causing buckling failure.

Figure 2.2 – Axial load vs. lateral deflection at mid-height (AD2), highlighting the occurrence of the first crack in the panel P2 (t = 125 mm) and the first crack in the panel P6 (t = 225 mm) (MUGAHED AMRAN *et al.*, 2019).

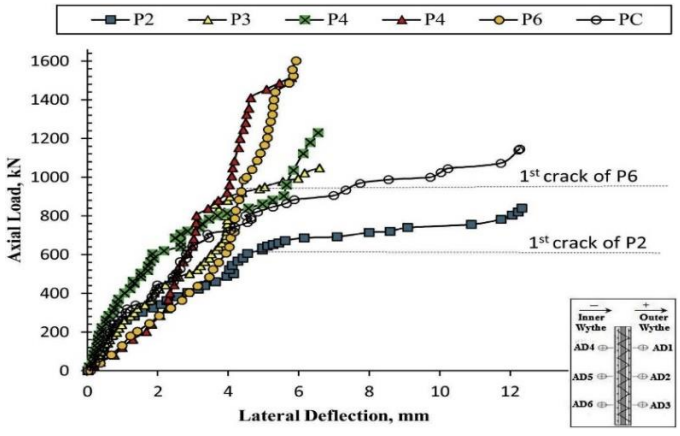

2.3.1.2 Materials

The failure of sandwich panels presents a predominantly brittle behavior. For this reason, researchers have been focused on strategies to induce ductile failure. Some materials used in such research are fiberglass, carbon, polyphenylene benzobisoxazole (PBO), PVA, and sisal fiber (DASKIRAN, DASKIRAN and GENCOGLU, 2020; FRANKL *et al.*, 2011; FRAZÃO *et al.*, 2018). Applying these fibers in the cement matrix reduces the compressive strength, but the gains in flexural strength explain the improved ductile behavior compared to conventional reinforced concrete wythes (DASKIRAN, DASKIRAN and GENCOGLU, 2016). Lee *et al*. (2018), for example, produced the wythes of their panels using a fiberglass mesh (GFRP) combined with high-performance fiberglass concrete (Figure 2.3).

Figure 2.3 – Face sheets applied to the composite sandwich panels; (a) ultra-high-performance fiber-reinforced; (b) glass fiber-reinforced polymer mesh; (c) glass fiber-reinforced polymer plate (LEE *et al.*, 2018).

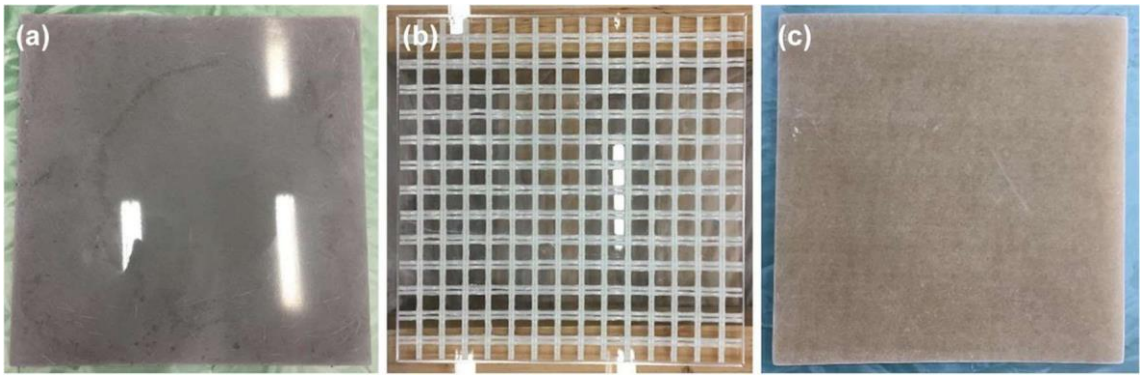

To understand the failure mechanism of this new material, Lee *et al*. (2018) performed a four- point bending test. The authors noticed that the prototype produced with the GFRP mesh showed a ductile rupture on the wythes where the mesh was applied and reduced weight (Figure 2.4). However, a reduction in the load capacity for this model was observed compared to the panel produced with a high-performance concrete wythe reinforced with 2wt.% steel fiber.

Figure 2.4 - Force vs. displacement curves in bending tests for composite sandwich panels: U-U1 - ultra-high-performance steel fiber concrete wythes; U-U2 - ultra-high-performance fiberglass concrete wythes (LEE *et al.*, 2018).

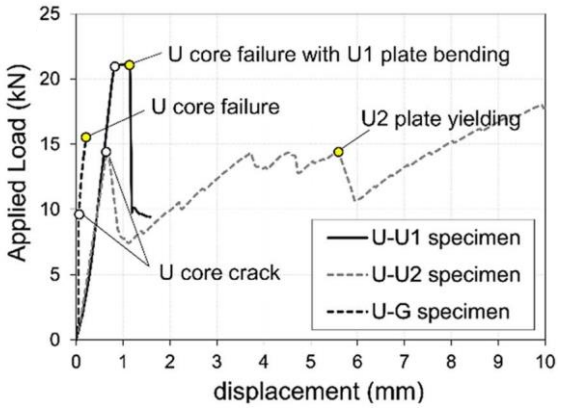

Mazhar *et al*. (2021) assessed the significance of multiple mesh layers in sandwich panels (Figure 2.5a; Figure 2.5b). The meshes impregnated with thermocol used by the authors were based on fiber cement to improve flexibility, durability and heat resistance. The results (Figures 2.6a and b) showed that the flexural strength of the prototypes increased by increasing the number of mesh layers.

Figure 2.5 - Sandwich panel with (a) four and (b) two layers of wire mesh (MAZHAR *et al*., 2021).

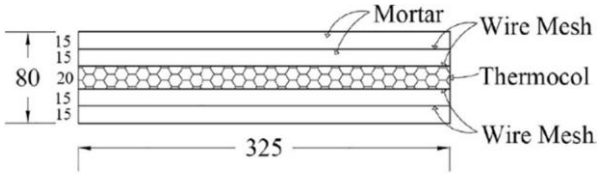

(a) Specimen A having four layers of wire mesh

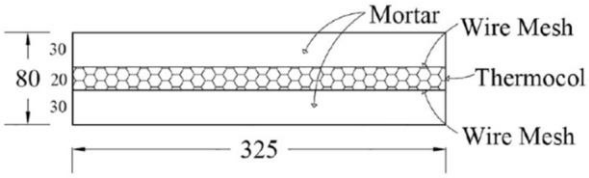

(b) Specimen B having two layers of wire mesh

Figure 2.6 – Load vs. displacement curves: (a) specimens with four layers of wire mesh under a two-point loading system; (b) specimens with two layers of wire mesh under a two-point loading system (AAMIR MAZHAR *et al.*, 2021).

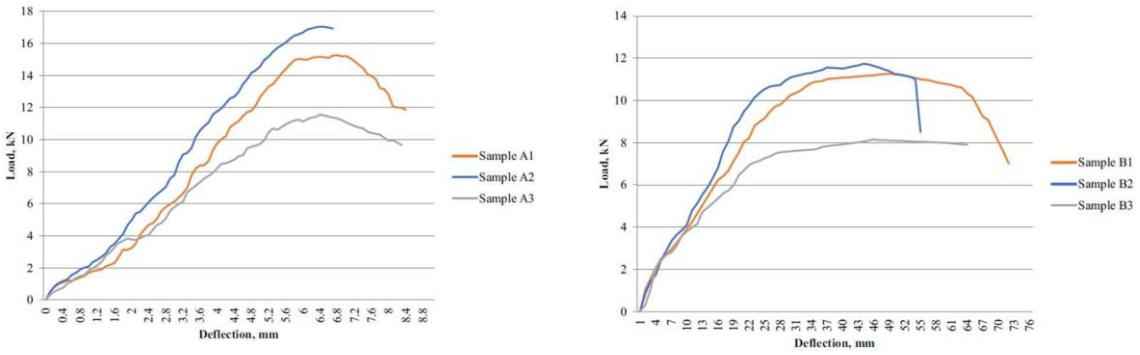

(a) (b)

2.3.2 Core

Recent studies have investigated the influence of the material, thickness and geometry of the core on the structural behavior of sandwich panels.

2.3.2.1 Core Materials

While the contribution of EPS core to the ultimate capacity of the panels is negligible (GARA *et al.*, 2012), new materials with different shapes and thicknesses seek to contribute to the structural capacity while maintaining a light structure (AHMED and ALI, 2020; OLUMOYEWA *et al.*, 2018; DUTRA *et al.*, 2019).

The materials used in the core have changed over time. Initially, the panels basically had Expanded Polystyrene (EPS), Extruded Polystyrene (XPS) and Polyisocyanurate (PIR) cores (PEČUR *et al.*, 2014). However, new solutions have been proposed and validated with the emergence of new materials and techniques. In this sense, vacuum-insulated cores, lightweight concrete, fiber concrete, mineral wool, and ferro-cement, among others, contribute not only to the thermal and acoustic properties but also to the ultimate mechanical performance (MAZHAR *et al.*, 2021; AHMED and ALI, 2020; O'HEGARTY and KINNANE, 2020b; PEČUR *et al.*, 2014).

Lee et al. (2018) studied the use of a lightweight concrete-based core with expanded polystyrene (EPS). The objective was to reduce the weight without reducing the ultimate

capacity. Silica fume was incorporated into the mixture to improve the adhesion between the EPS and the concrete, promoting gains in the bond between the EPS granules and the cement paste. This strategy increased the concrete strength about eight times compared to the mixtures that did not contain silica. The density was reduced from 2311.07 kg/m³ to 801.55 kg/m³ using the concrete with the highest EPS content.

The dosage study conducted by Lee et al. (2018), in which they replaced high-performance concrete with EPS based on bulk density, showed that the ideal EPS content in the mixture should vary from 30 to 40%. So, no marked reduction in strength was observed for a consistent reduction in the bulk density. Mixtures containing more than 50% EPS presented a highly porous matrix with less weight and greater thermal insulation capacity. The high-performance concrete produced by the authors, which was later applied to the panels, showed a density of 1550 kg/m³ and compressive strength of 60 MPa on the seventh day of curing.

CoDyre & Fam (2016), on the other hand, evaluated the application of foams with different densities in the core of sandwich panels. To this end, the authors used Polyisocyanurate (PIR) with different densities (32 kg/m³, 64 kg/m³ and 96 kg/m³) at the core of their prototypes. The results showed that by increasing the core density, there was an increase in the ultimate capacity when subjected to compression. For the densities of 64 and 96 kg/m³, the ultimate capacity increased by about 71% and 170%, respectively.

Comparing the counterparts A1/A4 and C1/C4 in (Figure 2.9), the authors realized that for the slendernesses investigated for both foam densities, the variation in global slenderness was not statistically significant for the ultimate load (Figure 2.9); i.e., comparing A1/C1 and A4/C4, it is noticed the positive influence of foam density on the loading capacity of the specimens. Also, a reduction in lateral deflections was observed by increasing the core density. This suggested a direct response to shear by increasing the foam density.

Figure 2.7 – Load (kN) vs. deflection (mm) (A1 – 750 mm; 32 kg/m³; A4 – 1500 mm; 32 kg/m³;C1 - 750 mm; 96 kg/m³; C4 – 1500 mm; 96 kg/m³) (CODYRE and FAM, 2016).

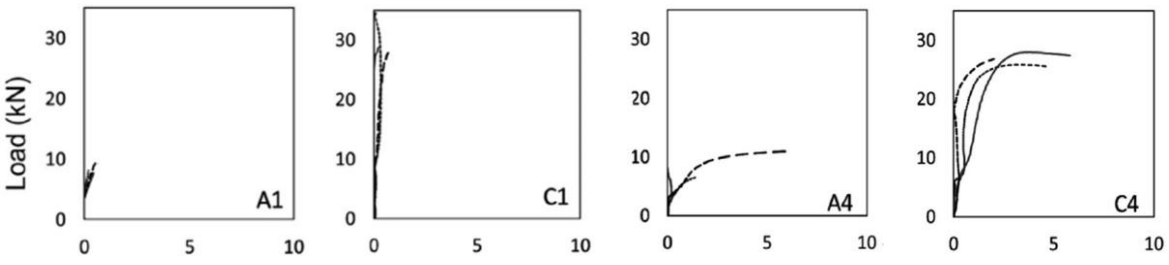

The ductile behavior of concrete can be improved by adding fibers to the composite. Ahmed & Ali (2020), for example, proposed the addition of 5% jute fibers 50 mm long (by cement mass) to produce concrete sandwich panels. Their results showed a good response in the impact strength test compared with conventional concrete. Adding jute fiber increased this value up to18%, allowing more significant deformations before the rupture of the panels.

2.3.2.2 Core thickness and geometry

In addition to the core's material, studies have shown that its shape, density and thickness are also parameters that directly influence the ultimate capacity of sandwich panels subjected to compression (AHN *et al.*, 2010; AKTAY, JOHNSON and KRÖPLIN, 2008; FISHER, 2008; RATHBUN *et al.*, 2006).

Dutra et al. (2019) produced panels with a honeycomb core based on epoxy, eucalyptus sawdust and cement. Their wythe sheets were produced with a piassava laminate (Figure 2.8).

Figure 2.8 - Sandwich panel model with piassava-reinforced sawdust core in honeycomb and rectangular shapes (DUTRA *et al.*, 2019).

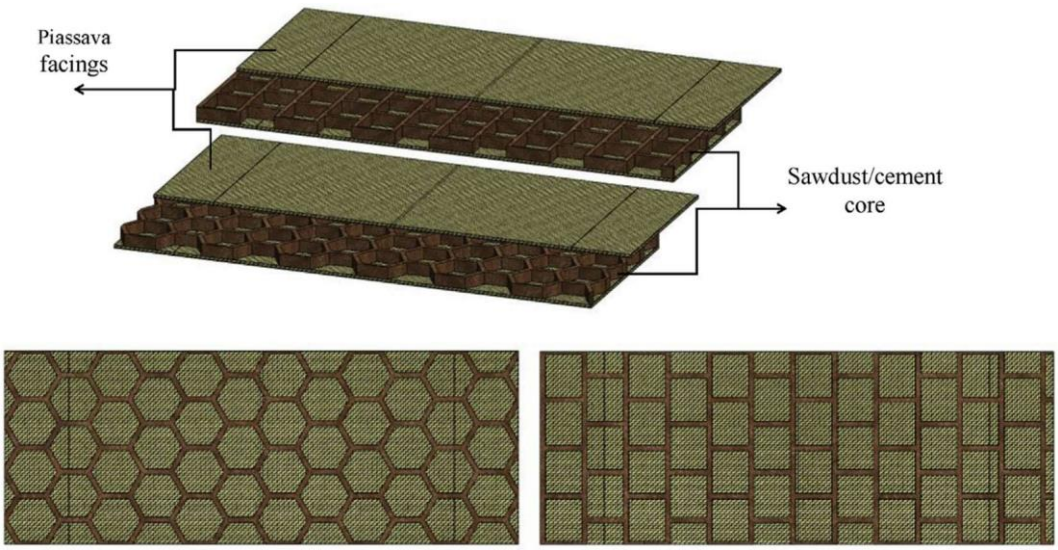

The authors performed a three-point bending test to evaluate the mechanical performance of this panel and noted that the ultimate capacity of the system increased by around 10 MPa (24%) by increasing the thickness of the honeycomb core and the density of the material.

This increase can be explained by the increased surface contact area and greater panel inertia, resulting in greater stiffness and stability.

Sarvestani *et al*. (2018) evaluated the impact behavior and buckling of cores produced by 3D printing in rectangular, hexagonal and auxetic shapes (Figure 2.9). The authors varied their densities and the angle of the cell wall in addition to the nuclei shape parameters. The auxetic sandwich panels absorbed more energy than the rectangular and hexagonal sandwich panels by 35% and 33%, respectively. The reason is that auxetic sandwich panels with higher densities need more impact energy to show large deflections and absorb more energy than the other shapes analyzed.

Figure 2.9 - Different 3D printed core shapes for sandwich panels evaluated by Sarvestani *et al*. (2018) (Height – 50 mm x width – 100 mm x thickness - 100mm): (a) Rectangular; (b) Hexagonal; and (c) Auxetic.

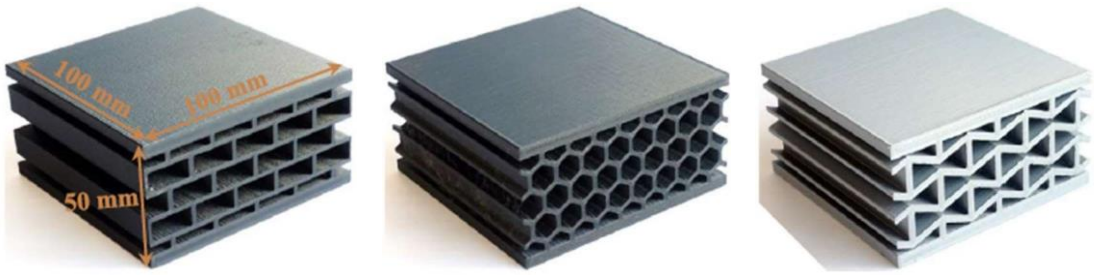

(a) (b) (c)

Mazhar *et al*. (2021) investigated the best impact behavior by producing a fiber cement core impregnated with thermocol (a product based on polyethylene and aluminum). The authors obtained load vs. displacement curves from the bending test results and observed a more significant response to deflection, showing a gradual increase until reaching its peak load. After that, the load gradually decreases, showing a ductile behavior. The use of thermocol between the wire meshes provided flexibility to the panel, restricting the propagation of small cracks and absorbing shock and loading.

Olumoyewa *et al*. (2018) also evaluated the incorporation of fibers in the matrix using steel fibers derived from discarded tires. Satisfactory mechanical strength was reached by adding 0.6% steel fiber to the lightweight concrete matrix. They noted that adding 0.6% steel fiber to the lightweight concrete matrix yielded satisfactory mechanical strength. The oxidation of Fe fibers to Fe oxides or hydrated oxides improves the adherence to the silicate matrix present

in the cement paste and increases the ductility of the matrix under loading. Adding steel fiber at a percentage lower than 0.6% reduced mechanical strength due to poorer adhesion and irregularities in the cement matrix.

Rejab & Cantwell (2013) compared the compression response of corrugated cores produced with glass fiber-reinforced plastic (GFRP) and carbon fiber-reinforced plastic (CFRP). In addition to evaluating different materials, they verified the influence of the number of unit cells (Figure 2.12a; Figure 2.12b). For both, the authors noticed that the structural behavior of the thick corrugated cores was close to that presented by aluminum honeycomb cores. Rejab & Cantwell (2013) noted that elastic buckling failure was predominant in all the evaluated panels.

Figure 2.10 - Corrugated-core sandwich panels based on aluminum alloy, a glass fiber reinforced plastic (GFRP) and a carbon fiber reinforced plastic (CFRP): (a) Damage in GFRP samples based on an increasing number of units cells, and (b) mold for production (REJAB and CANTWELL, 2013).

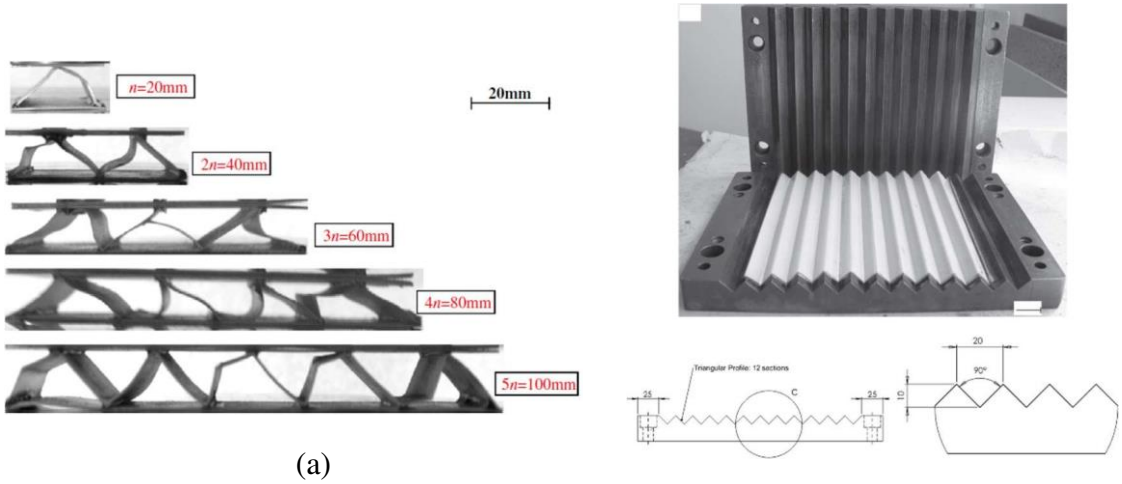

(a)

(b)(b)

A way to improve the buckling response of this corrugated core was presented by Yan et al. (2013). The authors inserted closed-cell aluminum-based foam into the core voids (Figure 2.11). The panels showed an increase in ultimate load and energy absorption capacity by 211% and 300%, respectively.

Figure 2.11 - Manufacturing process of sandwich panels with corrugated cores filled with aluminum foam (YAN *et al*., 2013).

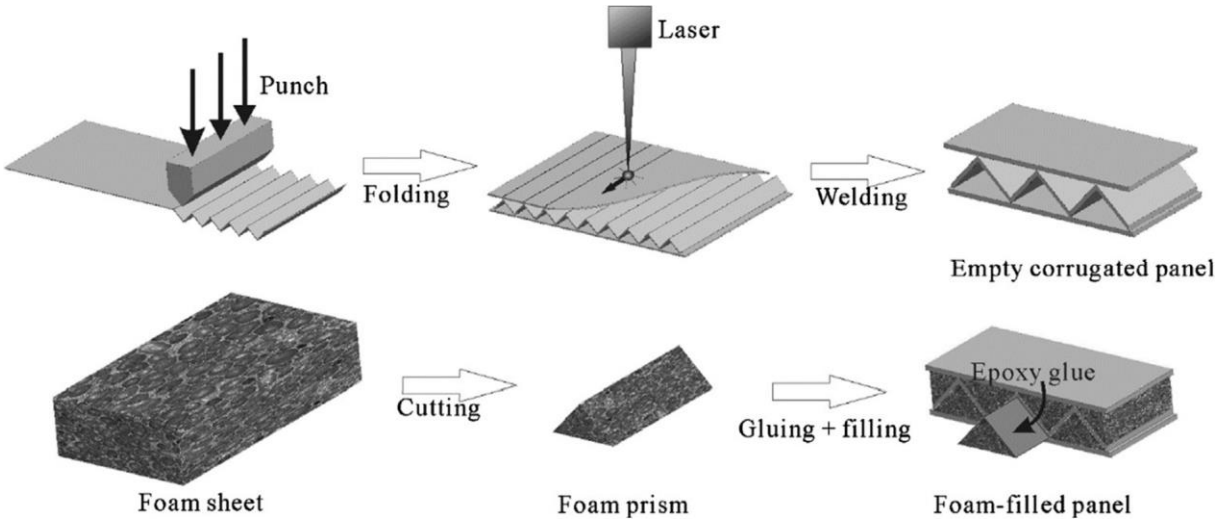

Damghani & Gonabadi (2016) evaluated the density variation of these foams in collaboration with corrugated cores. They found that the impact strength and the ductility of the system increased by 30% by increasing the foam core density.

Yang *et al*. (2017) reported that the energy absorption of corrugated panels also depended on the wall thickness of the corrugated core. Tests varying the thickness between 0.1 mm and 0.4 mm were conducted to confirm this. The authors noted that the global buckling capacity of the specimens with a 0.4 mm wall was six times greater than that exhibited by panels with a 0.1 mm wall.

A study on the effects of the number of corrugated cells on the compression response of sandwich structures was carried out by Zhou *et al.* (2016). They produced corrugated cores using carbon and glass fibers. To analyze the structural behavior of the panels, the authors varied the corrugation thickness and the number of unit cells.

The results showed that the number of cells for the tested nuclei had no notable effects (Figure 2.12). However, the results on thickness variation demonstrated similar behavior to those observed by Yang et al. (2017), showing that the compressive strength increased as the corrugation got thicker (Figure 2.13).

Figure 2.12 – (a) The four scaled sizes of CFRP core and (b) The influence of the number of unit cells on the compressive strength (ZHOU, GUAN and CANTWELL, 2016).

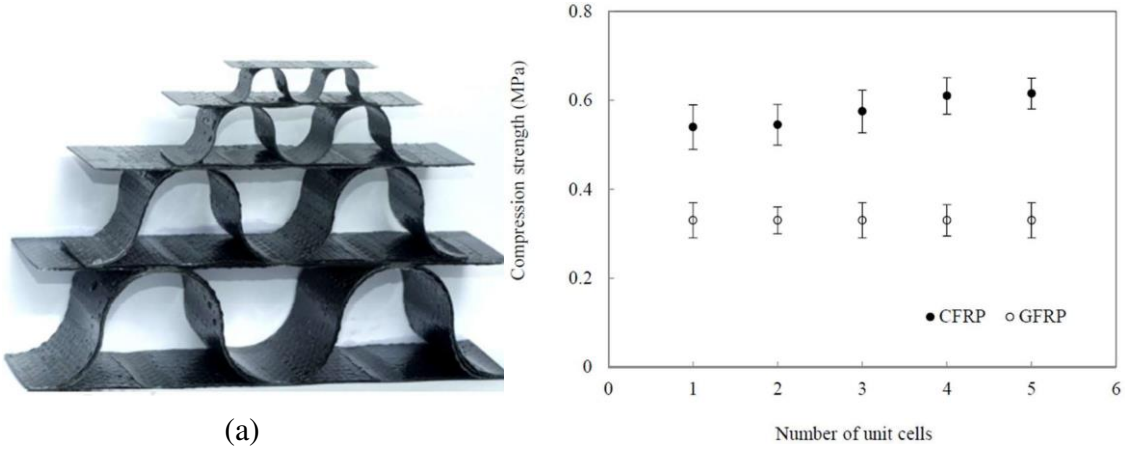

(a) (b)

Figure 2.13 – Compressive strength vs. strain curves for different corrugation thicknesses: (a) fiberglass core models GFRP and (b) Carbon fiber reinforced plastic (CFRP) (ZHOU, GUAN and CANTWELL, 2016).

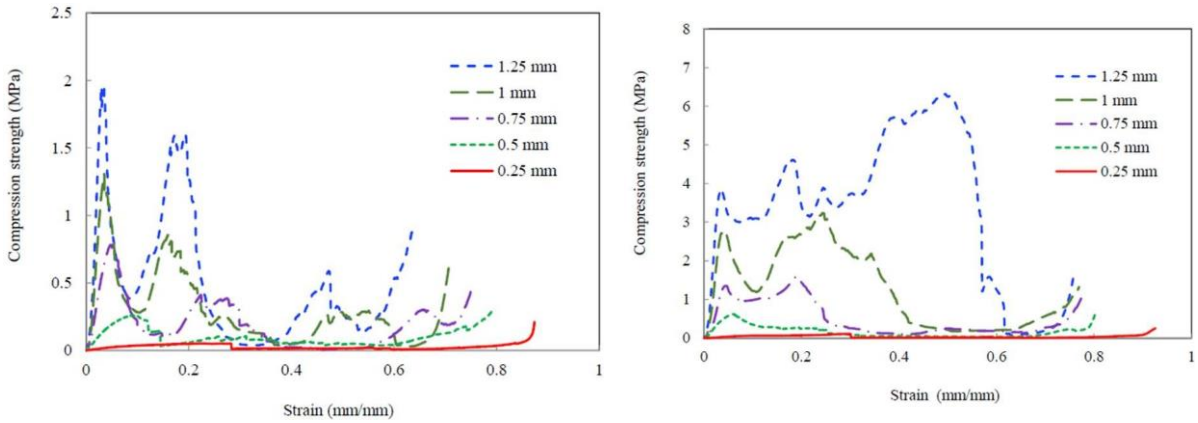

(a) (b)

2.3.3 Shear connectors

The shear connectors are crucial to connect the layers providing a composite behavior between the connected parts, which increases the load-carrying capacity and the local and global stability of panels (CUI et al., 2021). The most common connector is the lattice (ALCHAAR and ABED, 2020; BENAYOUNE *et al.*, 2007; AMRAN *et al.*, 2016); however, new models of shear connectors have also been proposed, varying not only the shape but also the material used (CHOI, KIM and KIM, 2015; FLANSBJER *et al.*, 2018; HOPKINS, NORRIS and CHEN, 2017; LAMEIRAS *et al.*, 2013).

According to O'Hegarty & Kinnane (2020), the deformations in panels with composite behavior are smaller and, therefore, the stresses. This shows that the composite work between the concrete wythes leads to designs with thinner walls for the same loading capacity (Figure 2.16a; Figure 2.16b; Figure 2.16c).

Figure 2.14 - Composite behavior levels of sandwich panels according to strain charts: (a)composite; (b) non-composite; and (c) partially composite (O'HEGARTY and KINNANE, 2020b).

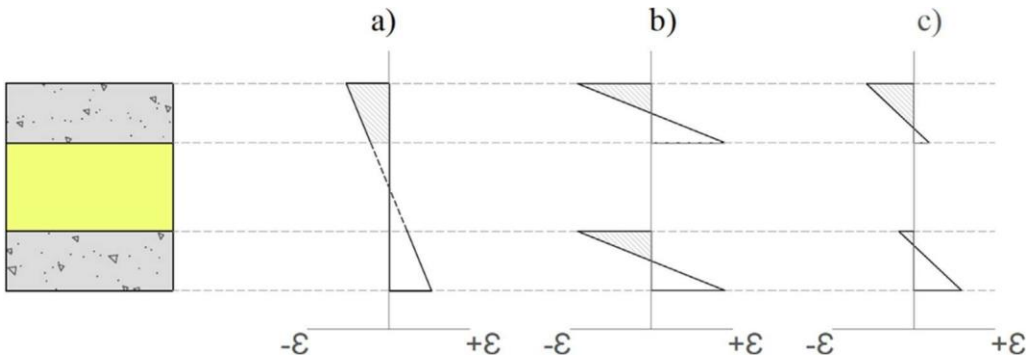

Shear connectors directly influence the composite behavior of sandwich panels. Graziani *et al*. (2017) evaluated the possible replacement of welded shear connectors with bent connectors, which makes production easier, reducing the need for skilled labor (Figure 3.15). The authors conducted axial and eccentric compression tests (Figure 3.15a) on the prototypes. The authors measured lateral deflection, vertical displacement and relative displacement between theconcrete wythes. Inclined displacement transducers were placed across the thickness of panels to measure the longitudinal and transversal components of the relative displacements between the two concrete wythes (Figure 3.15b; Figure 3.15c; Figure 3.15d). The welded connectors promoted greater composite behavior between the concrete wythes than the bent connectors. The results show that the welded connectors led to loads about 200 kN higher than the bent connectors in axial compression. However, it presented a worse behavior in eccentric compression than the bent connector. Panels with bent connectors presented an expansion of the core in the axial compression test due to the individual behavior of the sandwich layers (Figure 2.16a; Figure 2.16b).

Chen *et al*. (2015) produced new fiberglass connectors with three different shapes (Figures 2.19a-2.19c). The authors also compared the performance of their sandwich panels with a solid concrete panel (Figure 2.19d). The mechanical performance was assessed using four-

point and three-point bending tests. They observed that specimens with continuous (Group 3) and segmental (Group 2) connectors exhibited greater load-carrying capacity compared to discontinuous connectors (Group 1). Figure 2.20 shows that all the prototypes had a ductile response in all their configurations. In addition, the prototypes with continuous and segmental connectors obtained results close to the solid panels, with a slight loss of strength but presenting reductions in weight and cost.

Figure 2.15 – (a) Welded and bent shear connectors and (b) test setup (GRAZIANI *et al.*, 2017).

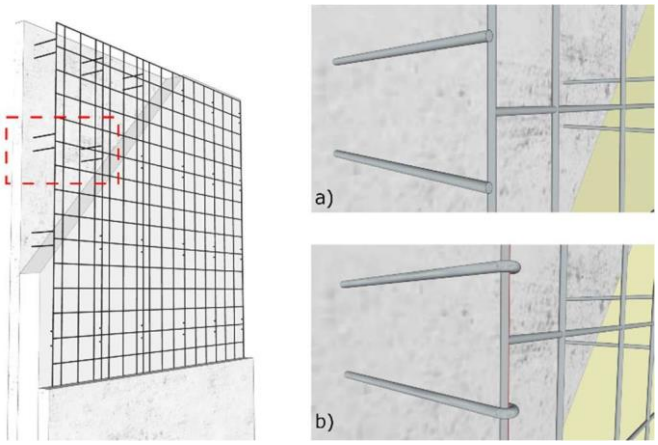

(a)

(b)

Figure 2.16 - Force vs. displacement curves obtained using welded and bent connectors: (a)A-1 (Folded connector) and A-2 (Welded connector); (b) E-1 (Bended connector) and E-2 (Welded connector) (GRAZIANI *et al*., 2017).

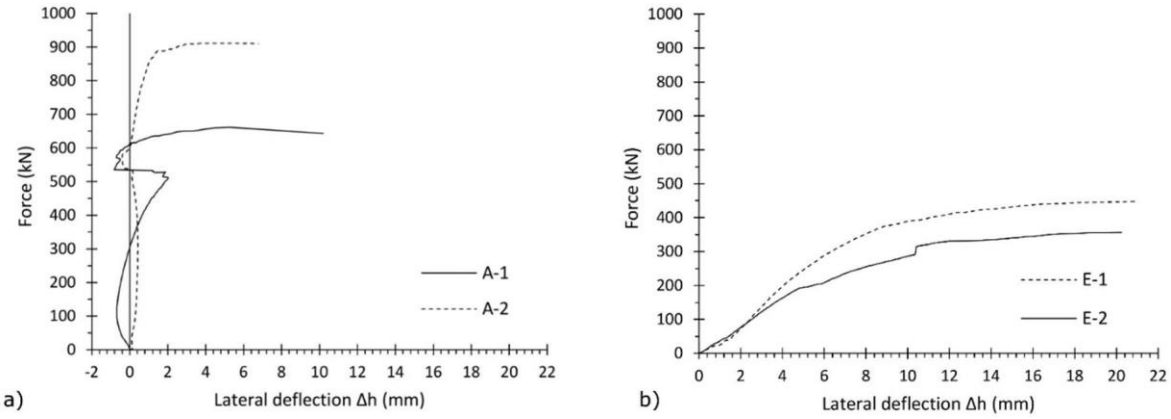

Figure 2.17 - Proposal of shear connectors: (a) discontinuous connector; (b) segmental connector; (c) continuous connector; and (d) solid panel (CHEN *et al*., 2015).

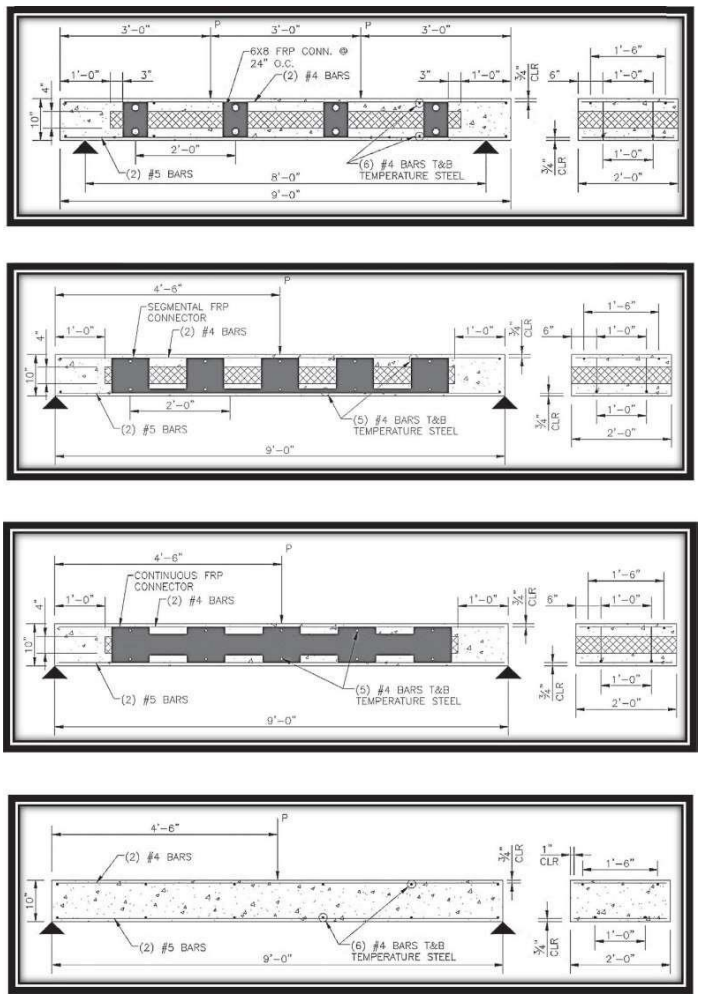

Figure 2.18 - Load vs. displacement curves obtained by Chen *et al*. (2015) for the different connectors evaluated.

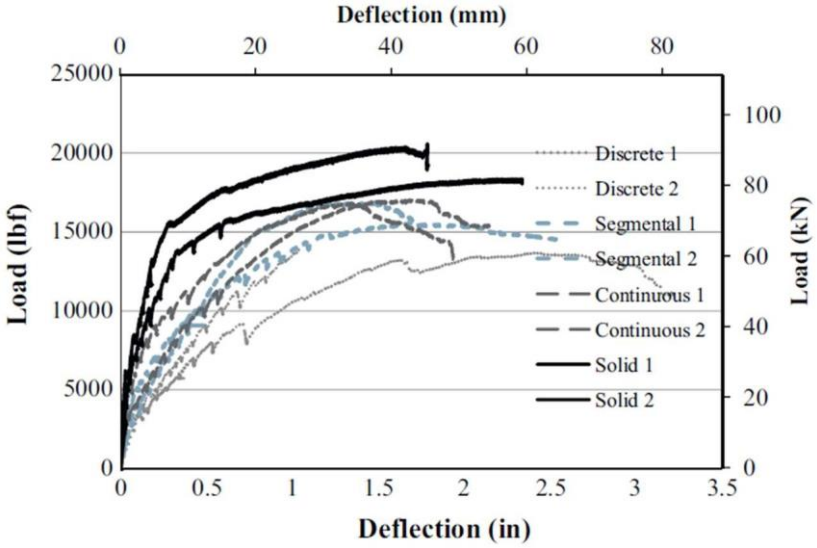

Alchaar & Abed (2020) evaluated the behavior of a lattice connector placed every 600 mm along the length of the panel. To evaluate the behavior of the composite, they used displacement transducers on both sides of the panel at different heights: 1000 mm, 2000 mm and 3000 mm from the bottom of the wall. Figure 2.19 show the load vs. displacement curves obtained. Both layers maintained the same lateral displacements at different heights during the linear behavior stage. Differences begin to occur in the nonlinear stage and continue to grow into the post-failure region.

Figure 2.19 – (a) Load vs. lateral displacement at mid-height of both concrete layers; (b) load vs. differential lateral displacement (DLD) between two concrete layers (ALCHAAR and ABED, 2020).

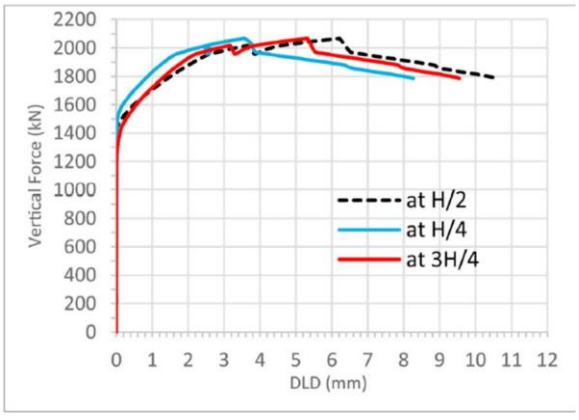

(a)

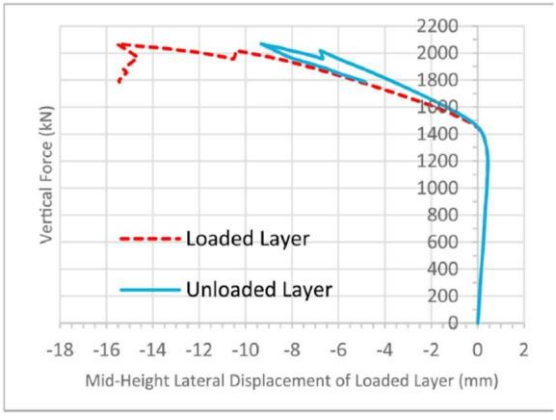

(b)

Qin *et al*. (2019) also used a lattice connector, proposing a new connector type for connecting the layers of the sandwich panels. The steel plate skin wythes served as formwork for the concrete core, working together to provide a composite behavior in service, supporting gravitational and lateral loads. The inner concrete layer increases the stiffness of the steel plate, preventing local buckling and increasing the flexural strength of the assembly, while the steel plates provide support to the concrete and increase its compressive strength (Figure 2.20). Compressive strength tests were carried out on three full-scale sandwich panels with different connector spacings: 200, 300 and 400 mm. The authors noted that panels with 400 mm spacing showed earlier local buckling and more severe bulges in the steel columns located at the edges of the panels. Local instabilities occurred between two adjacent steel connectors, showing that the steel lattice can be considered a boundary line for the steel plate for these composite panels. Panels with 300 mm and 400 mm spacing between connectors showed 18.5% and 25.9% lower ultimate strengths than the wall with 200 mm spacing. In addition, the initial stiffness was 7.3% and 10.7% lower than the 200 mm sample. The greater rigidity is due to the greater number of connectors and reduced spacing between them, offering a greater restriction to the external steel plate and improving the interaction between steel and concrete (Figure 2.21).

Figure 2.20 - Truss connector model surrounded by metallic sheet wythes (QIN *et al.*, 2019).

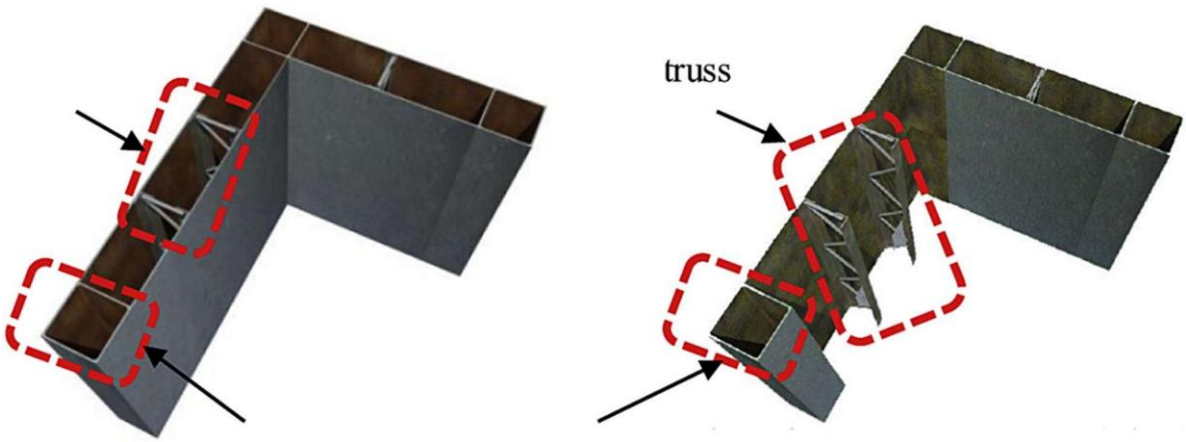

Figure 2.21 – Load vs. displacement for models with connectors spaced every 200 mm, 300 mm and 400 mm (QIN *et al.*, 2019).

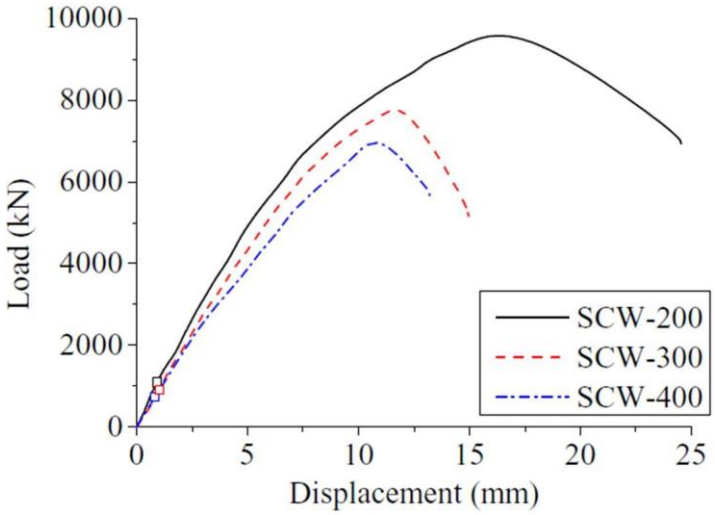

Tomlinson & Fam (2018) evaluated the interaction of bending moment and axial load in sandwich panels. For this, five panels were produced, one of which was submitted to the simple flexural test, one to simple axial compression, and three to an out-of-plane flexural load and, at the same time, different constant axial compression loads (C1, C2, C3) (Figure 2.24). The various axial load levels accompanied by mid-span bending effectively assess the composite behavior of the panels. Fam *et al*. (2018) evaluated this behavior using two methods: the composite action based on force (Equation 2.1) and the composite action through the slope (Equation 2.2). For Equation 2.1, M_u is the measured ultimate bending moment of the partially composite panel, and $M_{u,NC}$ and $M_{u,FC}$ are the non-composite and fully composite theoretical bending strengths, respectively. For Equation 2.2, I_{exp} is the inertia obtained experimentally, I_{FC} is the inertia of the theoretical composite behavior, and I_{NC} is the inertia of the theoretical non-composite behavior.

Figure 2.22 - Test setup and instrumentation for simultaneous flexural and axial compression loading experiments (TOMLINSON; FAM, 2018).

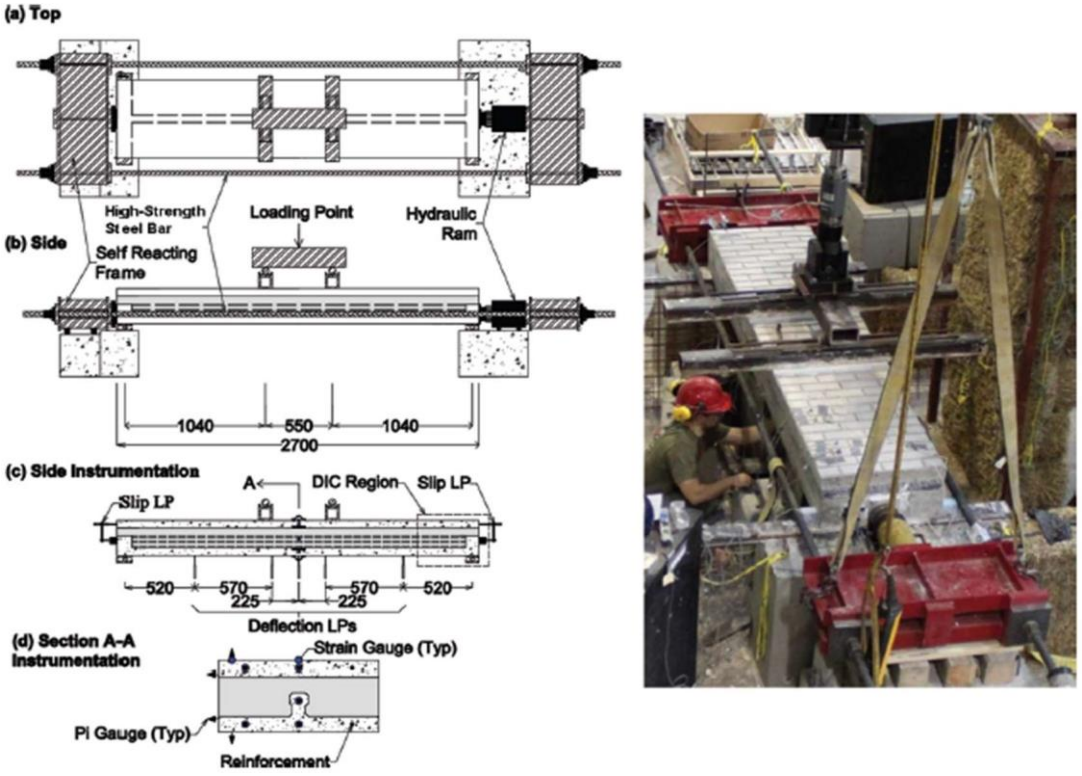

$$k_u = \frac{M_u - M_{u,NC}}{M_{u,FC} - M_{u,NC}} \; x \; 100$$

Equation 2.1 – Tomlinson & Fam (2018)

$$k_I = \frac{I_{exp} - I_{NC}}{I_{FC} - I_{NC}} \; x \; 100$$

Equation 2.2 – Tomlinson & Fam (2018)

The level of composite work based on force (k_u) decreased linearly from 87% to 11% as the axial load increased from 0% to 31% of the simple axial capacity of the structural wythe. On the other hand, k_I by the slope method was 5.8% on average, with the axial load not affecting the behavior. According to Tomlinson & Fam (2018), both analyzes should be considered for designing the connectors. They explain that a connector can have high stiffness and present a high value for k_I, but it can fail before reaching failure in bending, leading to a reduction in k_U. O'Hegarty *et al.* (2019) produced a new carbon fiber shear grid to be used as a connector. To evaluate a panel composite behavior, they used Equation 2.2 proposed by Tomlinson & Fam (2018). From the three-point bending test, the authors measured the displacement of the panels. However, they noticed that none of the four models produced showed a reasonable degree of composite behavior, obtaining results below 5%. This shows

that the connector produced by O'Hegarty *et al*. (2019) (Figure 2.23) is not providing sufficient strength to transfer the longitudinal shear forces between the top and bottom wythes in the thin panels during initial loading before failure. The insufficient stiffness of the insulation during bending deformation can explain such behavior.

Figure 2.23 - Shear connector breakage for sandwich panels produced with carbon fiber (O'HEGARTY *et al.*, 2019).

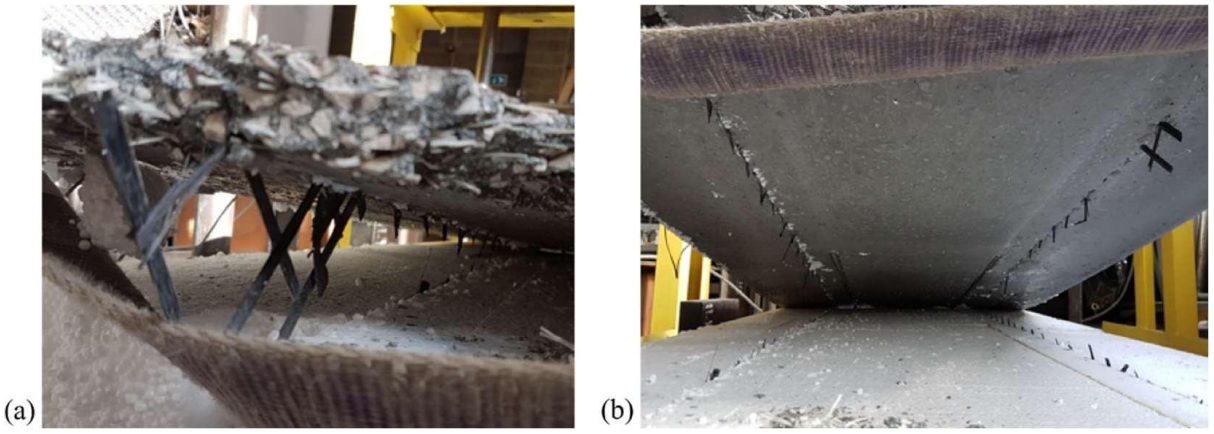

Flansbjer *et al*. (2018) produced a fiberglass lattice connector proposing two models: single and double (Figure 2.24). In order to evaluate the influence on the composite behavior, a bending test was carried out, and the panel sliding was measured. The study showed that the initial stiffness of the composite element is lower for the single connector than for the double connector. The first crack also occurred at slightly lower load levels. Upon reaching the maximum load, specimens with a single connector undergo a significant loss of stiffness represented by an almost horizontal line in the load vs. displacement graph (Figure 2.24c), which is believed to represent the connector pullout. The specimens with single connectors presented approximately 40% of the experimental flexural stiffness in the non-cracked stage and 57% of the load compared to the double connectors. In addition, the samples exhibited a relatively ductile failure even using a fragile material in the connectors.

Figure 2.24 – Shear connectors studied by Flansbjer *et al*. (2018): (a) and (b) fiberglass lattice shear connector; (c) load vs. displacement response (S-X: Simple Stretched Connector; D-X: Double Stretched Connector).

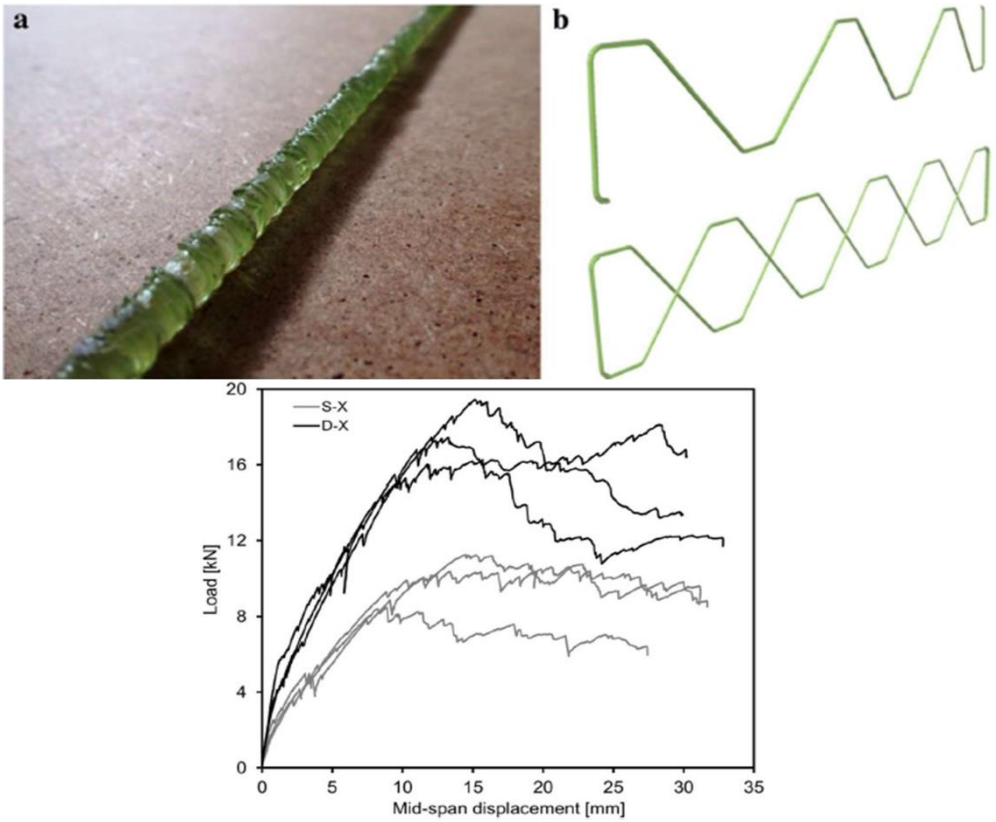

(c)

Lameiras *et al*. (2013) also evaluated three fiberglass shear connector types, two embedded in the concrete wythes and one bonded to the wythes by an epoxy adhesive (Figure 2.25). Their configurations were based on the perfobond and I-shaped connectors commonly used in composite steel-concrete structures (VALENTE and CRUZ, 2004). The pull-out test evaluated the failure modes, load capacity, stiffness, and connections capacity. The authors observed a greater slip corresponding to the rupture loads in the embedded connectors. In contrast, the adhesive-bonded connectors showed significantly less slip, which corresponds to the deformability of the adhesive layer and fracture propagation through the thin cement paste layer. For the perforated connectors, a relatively ductile failure occurred for all connections due to fiberglass failure near the holes (Figure 2.26a). For the embedded connectors, the failure was also ductile but showed a rapid progression of cracks on the surface of the blocks, followed by a sudden drop in load capacity (Figure 2.26b). The bonded connector showed the most fragile failure mode, with an incipient nonlinear branch before the peak load (Figure 2.26d).

Figure 2.25 - Cross-sectional scheme of investigated connections for sandwich panels: (a) embedded – simply perforated plate; (b) embedded – profiled; and (c) adhesively bonded (LAMEIRAS *et al*., 2013).

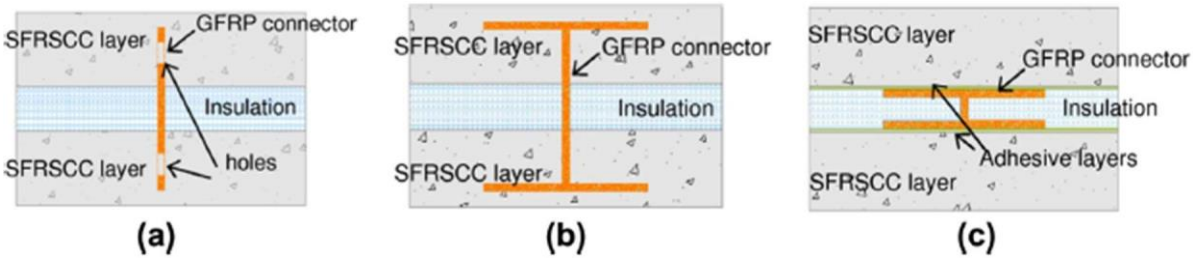

Figure 2.26 - Pull out test results: (a) perforated connectors with circular holes of 30 mm diameter; (d) perforated connectors with centers spaced 2d from each other; (b) connectors with elongated holes; (c) type I profiled embedded connector (d) Type I profiled adhesively bonded (LAMEIRAS *et al*., 2013).

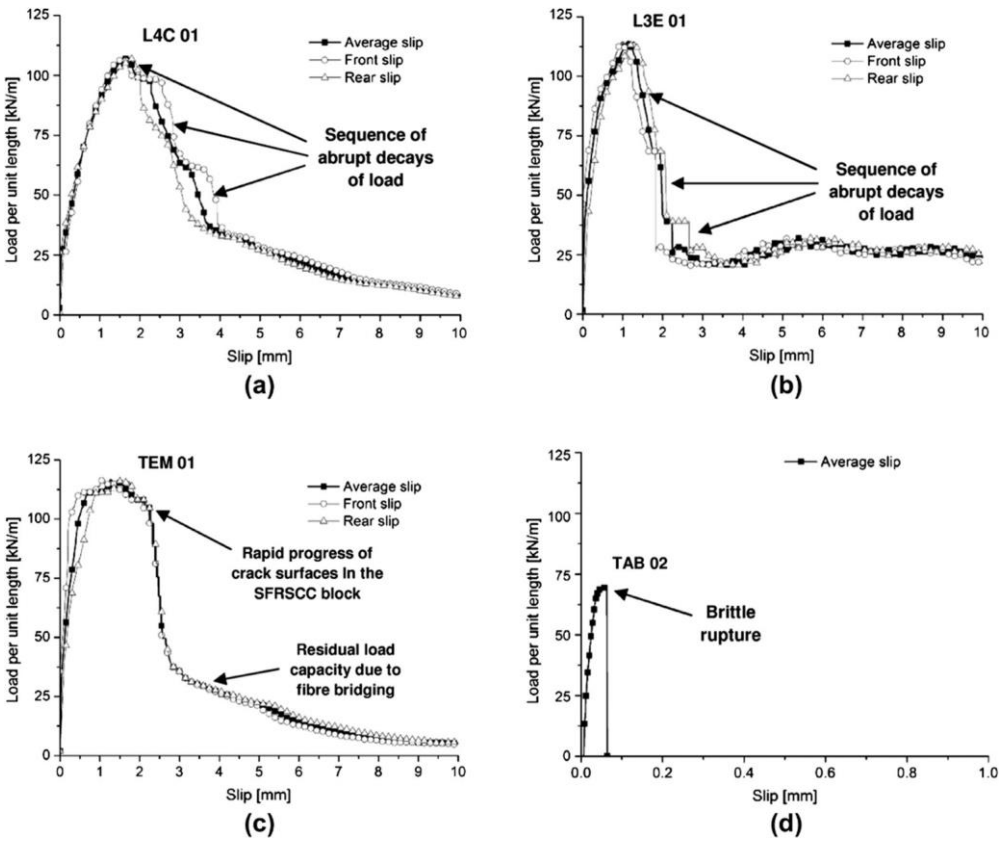

2.3.4 Global slenderness

The global slenderness, given by the height/thickness relationship, is an important parameter directly related to the failure mode of the panels. In order to investigate the influence of slenderness, Serpilli *et al*. (2021) produced six panels with two different heights, three 3000

mm high and three 1100 mm high. The authors obtained and evaluated the applied load vs. deflection curves (Figures 27a and 2b), observing non-representative out-of-plane displacement for the smaller panels, while two of the taller panels showed an out-of-plane displacement of up to 10 mm, causing a loss of stiffness in the specimens that led to a buckling failure. However, even with a slenderness 12, one of the prototypes had a very low displacement along with the test.

Figure 2.27 - Load vs. displacement curves for the (a) sandwich panel with a slenderness ratio equal to 12.5 (CC); and (b) sandwich panel with a slenderness ratio equal to 4.6 (CC) (SERPILLI; CLEMENTI; LENCI, 2021).

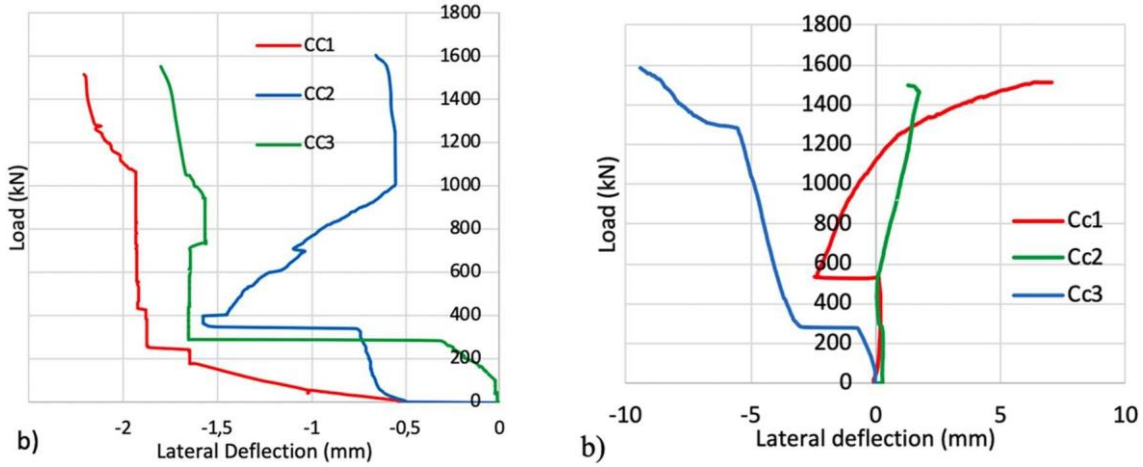

(a) (b)

Benayoune et al. (2007) produced panels with six distinct slenderness, ranging between 10 and 20They found a nonlinear decrease in strength as global slenderness increased. The ultimate load reduction for the extreme values of 10 and 20 was 21% (from 1425 kN to 1182 kN). The authors noticed a predominance of crushing at the ends of the panels. Several horizontal cracks along the panel were also observed in the slender prototype, attributed to the instability (buckling) of the panel. Figure 30 shows the measured out-of-plane displacements.

Unlike Serpilli et al. (2021), Mugahed Amran et al. (2016) noticed linear displacements for their prototypes, and as the height/thickness (h/t) ratio increased, higher displacements and lower peak loads were observed. Amran *et al*. (2016) presented graphs showing higher displacements at ½ height, with considerable displacements from slenderness 18 onwards (Figure 2.28). The authors also observed that the first cracks occurred approximately symmetrically on both sides. All the panels failed by concrete smashing (Figure 2.29).

Figure 2.28 – Load vs. displacement curves obtained by Amran *et al*. (2016): (a) at half height; (b) at 1/4 height from the upper end (GA1- h/t = 14; GA2 - h/t = 16; GA3 - h/t = 18; GA4 - h/t = 20; GA5 - h/t = 22; GA6 - h/t = 24; GAC - h/t = 24).

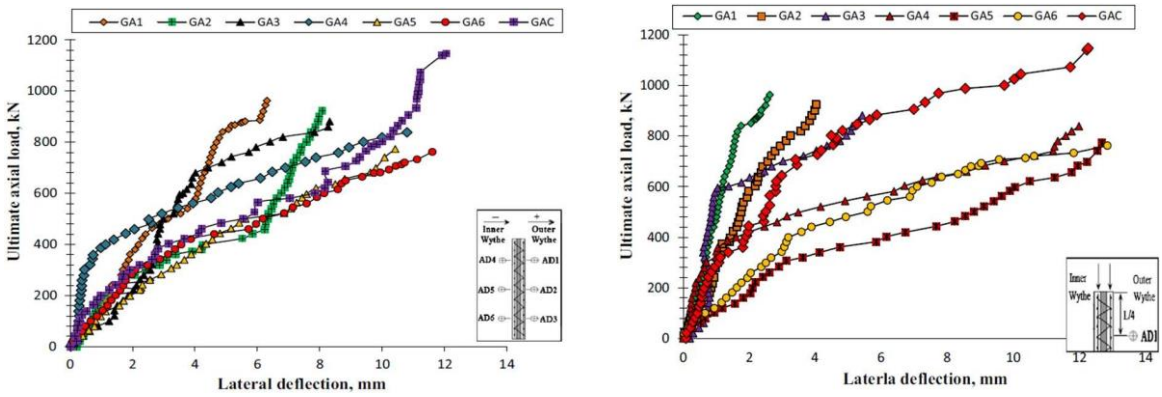

(a) (b)

Figure 2.29 – Typical concrete crush failure observed by Amran *et al*. (2016) (a) at the bottom end; and (b) at the upper end.

(a) (b)

Figure 2.30 – Results of (a) axial load vs. lateral deflection obtained by Benayoune *et al*. (2007) at 300 mm from the top of the specimens (PA1 – h/t = 10,77; PA2 – h/t = 11,67; PA3 – h/t = 13,85; PA4 – h/t = 15; PA5 – h/t = 18,46; PA6 – h/t = 20), and (b) comparison of the results obtained by the numerical and experimental analysis of the PA1 specimen.

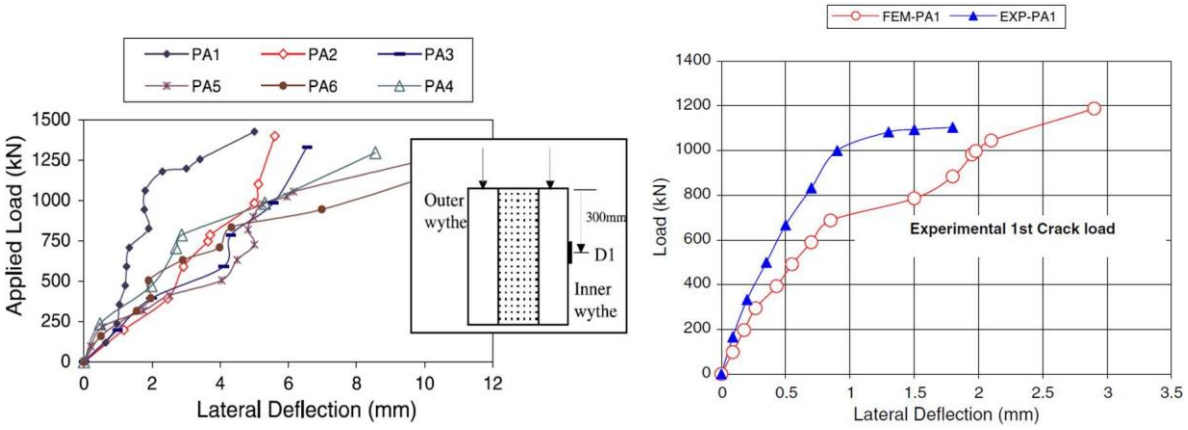

(a) (b)

The half-height displacement of the panel produced by Benayoune *et al*. (2007) with a slenderness of 10.8 differs from those observed by Amran *et al*. (2016) in their prototype with a slenderness of 14 and from those observed by Serpilli *et al*. (2021) in their prototype with the slenderness of 12.5. These two obtained low displacements for such slenderness, showing that for buckling instability in the center of the specimen, slenderness values above 20 are required.

Gara *et al*. (2012) evaluated panels under axial and eccentric compression to assess the influence of eccentricity on buckling failure. For the axial compression test, the final load of the panels is strongly influenced by small eccentricities generated in the production of the panels or even in the test configuration. However, even with a slight eccentricity, the behavior of the panels is still quite different compared to the eccentric compression test. In particular, the lateral deflections of the panels generally remain small until they reach values close to failure in axially loaded samples. For the eccentric test, the concrete layers behave differently from the beginning. While one layer suffers a shortening, the other elongates, causing failure predominantly by buckling the wythe (Figure 2.33). The results show that the influence of slenderness for the axial compression test is more significant than the presence of thicker cores; however, for the eccentric compression test, the panels suffered greater displacements and, at the same time, showed greater load capacity when increasing the core thickness (Figure 2.32).

Figure 2.31 - Prevalence of failure in sandwich panel specimens subjected to different load modes: (a) post-failure axial loading; (b) eccentric axial loading after failure; and (c) Mesh failure (GARA *et al.*, 2012).

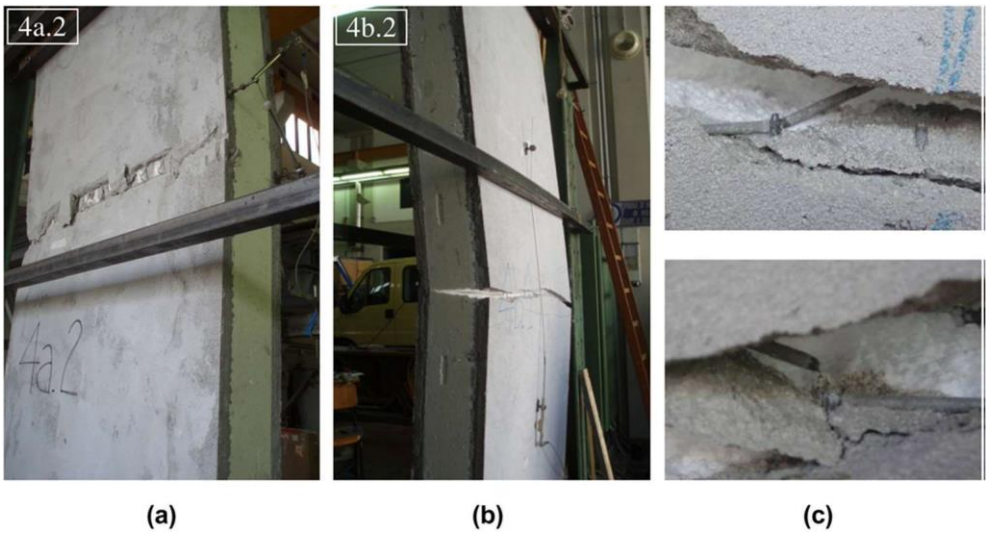

Figure 2.32 – Load vs. lateral deflection curves obtained by Gara *et al*. (2012) (WP08 – h/t = 19,6; WP12 - h/t = 15,47; WP16 – h/t = 12,78; WPN08 – h/t = 19,6; WPH08 – h/t = 19,6; a.1, a.2 = axial load; b.1, b.2 = eccentric axial Load).

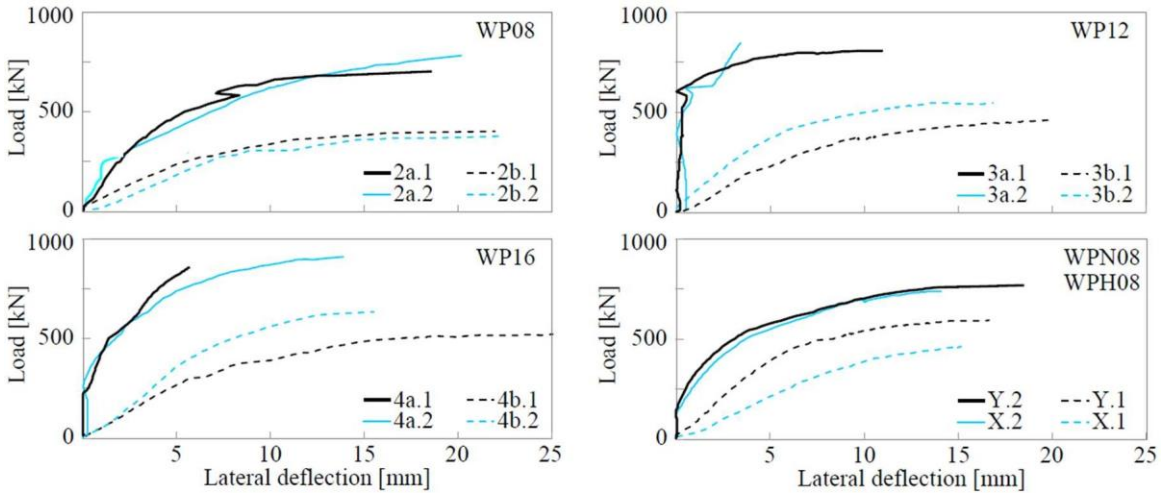

Qun *et al*. (2018) studied sandwich panels with slenderness up to 21.8. However, to mitigate the buckling effect, they proposed a model with columns confined by spiral stirrups arranged every 600 mm, a double layer of mesh welded on the wythes, and a three-dimensional steel wire skeleton (Figure 3.33). The results show that the panels produced with the three-dimensional steel wire skeleton reached a load capacity three times greater than the control panel (Figure 3.34).

Figure 2.33 - Sandwich panel model with pillars along the length and double-layer mesh on the wythe (QUN; SHUAI; CHUN, 2018).

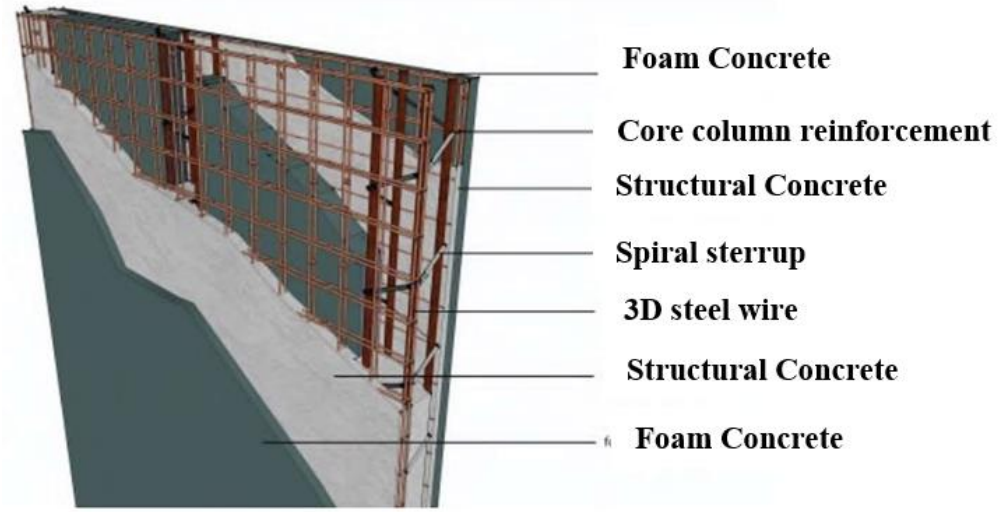

Figure 2.34 - Load vs. deflection curves obtained by Qun *et al*. (2018): (a) ZY-1 = planar model with only one mesh layer (h/t = 21.82); (b) ZY-2 = model with a double mesh layer on the two concrete wythes (h/t = 17.1).

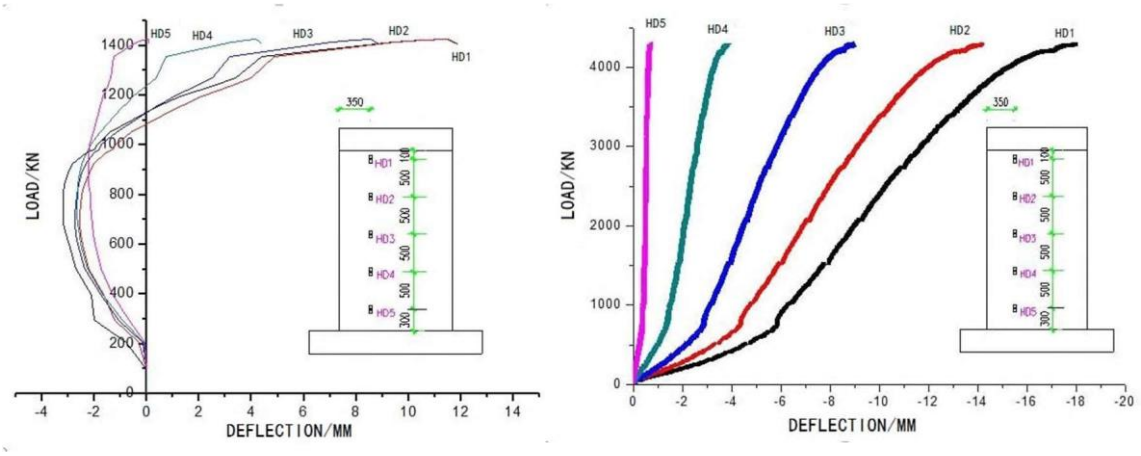

(a) (b)

2.4 Analytical models

Over the years, authors have produced empirical equations to predict the load-carrying capacity of sandwich panels subjected to compression loads through laboratory studies and finite element analysis.

Amran *et al*. (2016) evaluated the application of five equations produced by other authors to predict the ultimate axial compression load for their sandwich panels. The authors produced six panels with different slenderness ratios, obtaining load vs. slenderness graphs (Figure 2.35). Through the graphs, Amran *et al*. (2016) managed to produce an accurate equation for their panels (Equation 2.3). The authors showed that the equation proposed by the American Concrete Institute underestimates the load resisted by their panels, while the one proposed by Parthasarathy (1977) overestimates the load (Seeber *et al*., 1997). The first leads to a less cost-effective dimensioning, while the second can produce an unsafe solution.

$$P_u = 0.37 f_{cu} A_c \left[1 - \left(\frac{kH}{32t}\right)^2\right] + 0.67 f_y A_s$$

Equation 2.3 –Amran *et al*.(2016)

Figure 2.35 - Results of different prediction equations compared to the experimental and numerical results of Amran *et al.*(2016).

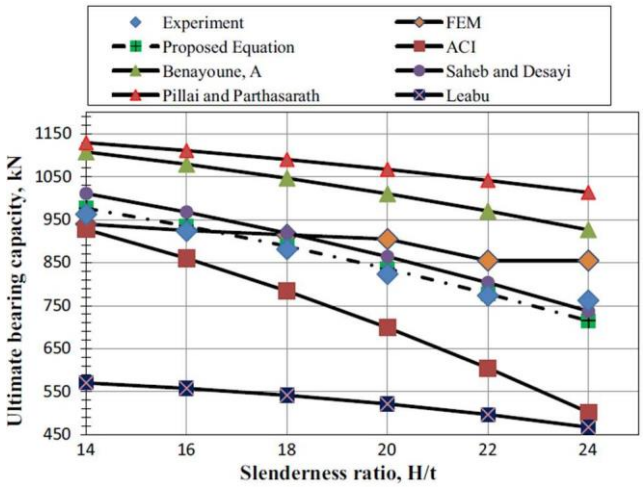

The parameters used by Amran *et al.* (2016) were based on equations proposed by other authors. The first parameter refers to the strength of the concrete wythe, considering the gross area of the cross-section (A_c) and the characteristic strength of the concrete (f_{cu}) multiplied by a constant equal to 0.37. However, since slenderness influences the concrete contribution, it was multiplied by a factor that considers the type of constraint at the ends (k), the height (H) and the gross thickness of the model (t). The contribution of steel is summed, considering the steel area (A_s) of the rebars, which contributes to the compressive strength and the yield strength (f_y) of the steel used in the prototype.

Mugahed Amran et al. (2016) also showed that the influence of the height/thickness ratio in sandwich panels is a parameter of great influence on the ultimate capacity. However, in their equation, they did not use the effective thickness of the panel, i.e., they consider that the EPS core participates in the compressive strength of the panels. This discussion was raised by Gara *et al.* (2012), that performed shear testing on smaller prototypes of sandwich panels to assess the ultimate capacity (Figure 36a). The latter showed that the influence of the core on the panel strength is insignificant (Figure 36b); however, they did not evaluate different core thicknesses but only confirmed that the removal of the core did not cause a reduction in strength for their prototypes.

Figure 2.36 – Tests performed by Gara *et al*. (2012) in reduced prototypes: (a) Shear test; (b) load vs. displacement curves (1S - H = 80 mm with EPS; 3S - H = 160 mm with EPS; 5S – H = 80 mm without EPS).

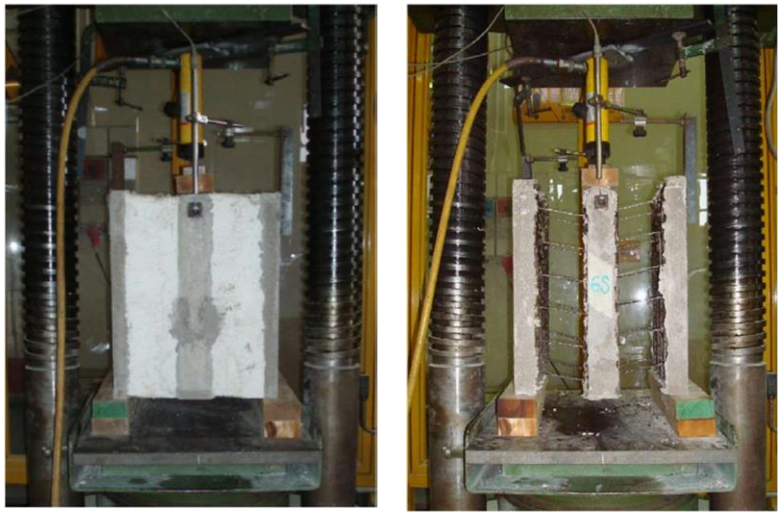

(a)

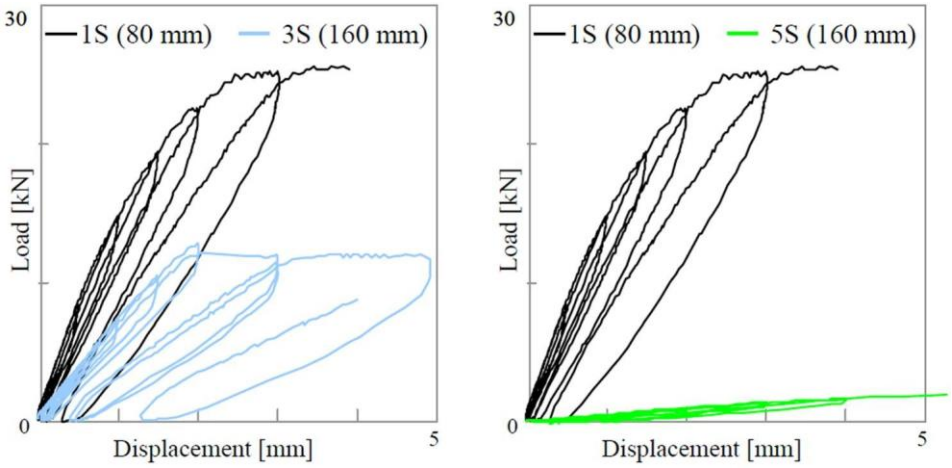

(b)

Carbonari et al. (2013) evaluated the influence of the core thickness on the ultimate capacity of panels. The authors observed that as the core thickness increased, the ultimate capacity reduced, while the variation in the thickness of the mortar layers did not influence the ultimate capacity. Apparently, the increase in cross-section does not affect the failure mode, which is more dependent on the EPS thickness (length of the connectors) and the compressive strength of the concrete layers (Figure 2.37).

Figure 2.37 - Failure modes in sandwich panels: (a) due to combined compression-flexion; and (b) due to lateral instability (CARBONARI *et al.*, 2013).

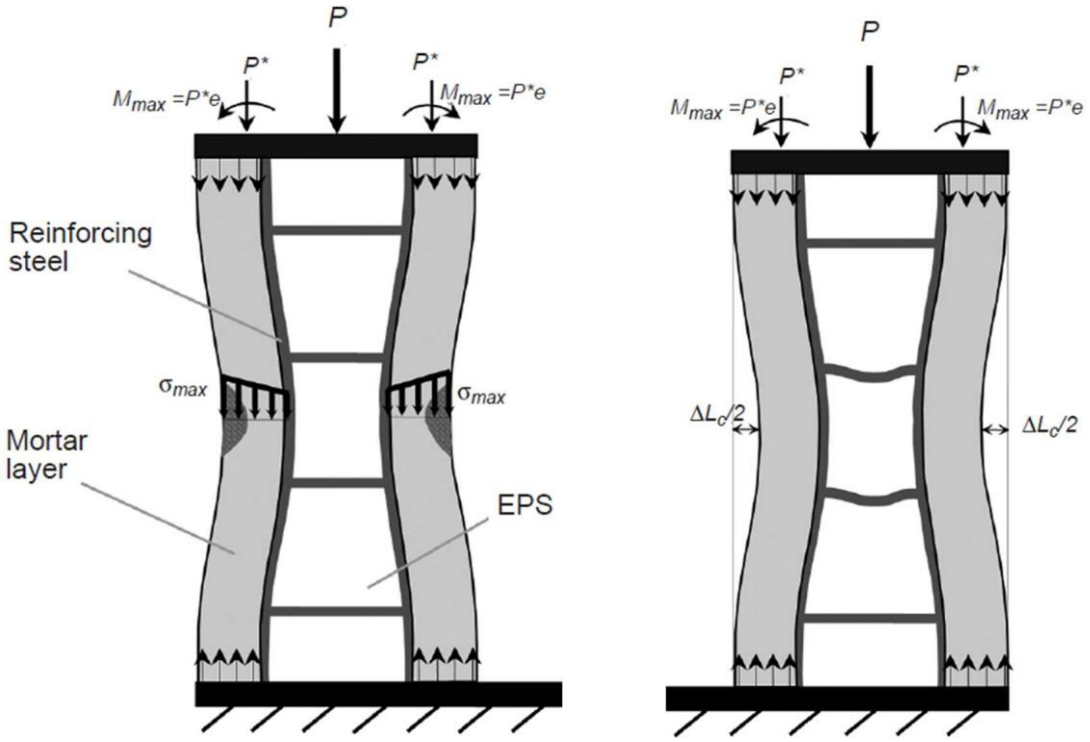

According to Carbonari *et al.* (2013), if the failure is caused by lateral instability, it is advisable to increase the number or diameter of the shear connectors to improve the maximum load capacity. However, if the failure is caused by concrete crushing, it would be better to change the thickness of the mortar layer or the material's mechanical strength.

Carbonari et al. (2013) based their analysis on Euler's hypotheses, with failure due to lateral instability observed when the lateral displacement in the center of the panel is equal to half the displacement necessary to produce buckling in the connectors. To present this mathematically, they used Equation 2.4, where k_1 and k_2 are the coefficients representing the panel boundary condition (ranging from 0.5 for fixed ends to 1 for pinned ends). The coefficient k_3 (ranging from 0 to 1) considers the restriction produced by the EPS core and the connectors. L_c, ϕ_c and $n_{c,secc}$ represent the length, diameter and number of steel connectors per horizontal line for a certain eccentricity (e). In addition, the buckling height ($L_{buckling}$) is considered to be half of the actual length of the panel, while E_m and I_{layer} represent the modulus of elasticity of the concrete and the moment of inertia of the material. Thus, Carbonari et al. (2013) were able to more accurately predict the mechanical behavior of their models,

unlike Amran *et al*. (2016), who proposed an equation restricted to their panel type.

$$P^{*}_{max} = \frac{8E_m I_{layer}}{k_2^2 L^2_{buckling}} \left[\operatorname{acos}\left(\frac{1}{1 + \frac{n_{c,sec}\pi^2\varphi_c^2}{32e\,k_3 k_1^2 L_c}} \right) \right]^2$$

Equation 2.4 - Carbonari *et al*. (2013)

2.5 Conclusion

The authors consider that industrialization in the construction sector has a critical role in solvingthe housing and infrastructure deficits in developing countries and being critical in improving quality of life and social, economic and environmental sustainability. A review of sandwich panels is presented in this article, focusing on mechanical performance (markedly compressive strength) and addressing behavior, experimental programs, the influence of the parts on the global behavior and prediction equations for structural design. Advances in materials and technologies were also presented and discussed.

Both the shape and the arrangement of the connectors influence the structural efficiency, promoting greater or lesser composite behavior. Meanwhile, concrete wythes have been produced with the application of new materials of increasing applicability, such as glass and carbon fibers, thus avoiding durability problems related to the corrosion of steel rebars. Recent research has evaluated different cores aiming to reduce weight without impairing the mechanical capacity, varying both material and shape, showing that they can also promote gains in mechanical performance, reducing weight, and providing good thermal and/or acoustic performance.

Analytical equations that describe the behavior of these panels with good accuracy have been proposed, considering not only the influence of the global slenderness but also the thickness of the core, the spacing between connectors, the diameter and thickness of the concrete layers, and the influence of the reinforcement.

This review of recent studies consists of a relevant contribution to expanding research on the subject and promoting such technologies for application on an industrial scale in both developed and developing countries. For this, the authors also encourage expanding research

on eco-efficient and alternative materials applied in such solutions, as well as production in small local businesses for application in developing countries.

CHAPTER 3. Compression behavior of a new typology of concrete sandwich panel

Abstract

The first patent for precast concrete sandwich panels with shear connectors (PCSP) was registered in 1986. Since then, experimental studies have investigated innovations for applications of new materials and adaptations in geometry. Recent research has addressed the influence of sandwich panel parts for different configurations, including different shear connectors, core materials and geometries on the load-carrying capacity of sandwich panels. The objective of these studies has been the development of a typology that presents a better ultimate capacity/weight relationship compared to the traditional PCSP setup. Global bucklingand concrete wythe crushing are the main failure modes exhibited by the PCSP used as a wall system. For this research, a sandwich panel typology with longitudinal ribs was used and evaluated for axial compression. The ribs played a role in contributing to an improvement in rigidity without significantly impacting the panel's self-weight.

3.1 Introduction

The first patent on precast concrete sandwich panels (PCSP) was registered by Tadros et. al. (1995) in 1995. This consists of a sandwich of two concrete wythes interspersed by a lightweight foam core, in which steel shear connectors are used to connect the concrete wythes (AHMED; ALI, 2020b; ALCHAAR; ABED, 2020b; ATOYEBI OLUMOYEWA *et al.*, 2018).

Over the years, new typologies and materials used for shear connectors have been proposed and evaluated. (BAI and DAVIDSON, 2015b; GRAZIANI *et al.*, 2017; QIN *et al.*, 2019b). The main purpose of this component is to connect the wythes so they can work together. Equations to predict the degree of composite behavior between the wythes have been proposed, such as those by O'Hegarty *et al*. (2019) and Tomlinson and Fam (2018).

New composite materials with mechanical strength comparable to steel have been studied in sandwich panels. These components provide improved thermal conductivity and resistance to aggressive agents, bringing additional benefits when compared to steel shear connectors (FLANSBJER *et al.*, 2018; O'HEGARTY *et al.*, 2019b). Flansbjer *et al*. (2018) studied lattice-type shear connectors made of fiberglass. It was observed that the composite structural behaviorof the concrete wythes was considered highly dependent on the stiffness and strength of the connectors. The modulus of elasticity found for the fiberglass rebar was 40.3 GPa, five times lower than the modulus of steel commonly used in civil construction. As the material's modulusof elasticity is directly linked to stiffness, the panels with steel shear connectors exhibited greater behavior comparate to those of fiberglass rebar connectors.

O'Hegarty *et al*. (2019) produced carbon fiber grid connectors. The experimental results, however, showed very little evidence that the shear grid improved the composite behavior of the panel. All panels showed degrees of composite behavior of less than 5%. However, unlike the predominantly fragile failures of panels with steel connectors, the panels with carbon fibergrid connectors exhibited significant post-crack strength, showing ductile behavior and resulting in an overall ductile failure.

The materials used in the wythes have also been studied and improved. This part of the panel

directly influences the structure stiffness due to the inertia of the wythe. O'Hegarty et al. (2019), for example, increased the concrete outer layer thickness from 25 to 40 mm, which increased the total thickness of the panel by 10% (from 155 mm to 170 mm). The total panel weight increased by 20% but doubled the load-carrying capacity and bending stiffness.

Lee *et al*. (2018) tried to reduce the self-weight of the prototypes using panels with fiberglass wythes (SPEPC). The results showed a ductile behavior on the wythes, in addition to responding with greater stiffness and avoiding out-of-plane buckling. The specimens with fiberglass wythes supported 15 kN more than those with concrete wythes and expanded polystyrene (EPS). Another advantage is that the latter failed by buckling, while the fiberglass wythe could transfer the failure to the EPS concrete core, practically remaining in its initial position.

The lightweight core initially did not focus on mechanical performance. It had only the role of improving the thermal performance and reducing the structure's self-weight. However, recent studies investigated the application of new core materials and geometries able to contribute to the load-carrying capacity (DUTRA *et al*., 2019b; SARVESTANI *et al*., 2018b; ZHOU, GUAN and CANTWELL, 2016b).

The evaluation of the typology and materials used on the core and wythes on the structural behavior of the panels is based on experimental tests. Depending on the different actions, and consequent failure modes, sandwich panels can be evaluated in simple bending, diagonal compression and axial and eccentric compression (JOSEPH *et al*., 2018b; GARA *et al*., 2012b; AMRAN *et al*., 2016).

Simple bending tests are commonly conducted on sandwich panels since the bending test provides a better response regarding composite, semi-composite and non-composite behavior. Experimental results of bending tests are more commonly found in the literature (CHEN *et al.*, 2015; CHOI; KIM; KIM, 2015; LEE *et al.*, 2018; O'HEGARTY *et al.*, 2019).

The diagonal compression tests aim to study the shear behavior of the panels since the shear is nothing more than a traction effort in the transverse direction of the crack (AHMAD and SINGH, 2021; SERPILLI, CLEMENTI and LENCI, 2021). This test measures the elongation and shortening to gauge its shear performance. Axial or eccentric compression tests evaluate

panels' performance to gravitational loads when applied to structural walls or thermal protection of buildings' facades. (BENAYOUNE *et al.*, 2007; JOSEPH *et al*., 2018b; GARA *et al.*, 2012b; AMRAN, *et al.*, 2016).

Compressed panels fail predominantly by concrete wythes crushing, wythes or shear connectors localized buckling. Recent studies have evaluated the influence of global slenderness on thin panels. Carbonari *et al*. (2013) evaluated the axial performance in reduced prototypes and noticed that the core thickness does not directly affect the strength. However, the greater the thickness, the greater the distance between the wythes, consequently, the greater the connector's width, which can result in premature shear buckling. For high widths, the connectors fail by localized torsion, thus reducing the final strength. The strength of the mortar used on the wythe is another parameter that Carbonari *et al*. (2013) pointed out as being of great influence in their studies since the greater the strength, the greater the structure stiffness.

On the other hand, Amran *et al*. (2016) varied the panel's height and reached global slendernessup to 24. Unlike other authors, even with high slenderness, the models failed by concrete wythes crushing at the ends of the panels. For global slenderness greater than that, the ultimate capacity of the prototypes was reduced by up to 26%. Another study by Serpilli *et al*. (2021) showed that accidental eccentricities caused premature failures in their prototypes. They also noticed that the failure mode was similar to those obtained in classical structural masonry, where diagonal cracks are formed at the load application point. Meanwhile, Qun *et al*. (2018) noticed brittle behavior and a vertical crack along with the entire height of their model, with considerable concrete crushing at the top of the panels.

Understanding the behavior of panels under compression is extremely important for adequately designing the panels used as structural walls. To the authors' knowledge, the compressive behavior of sandwich panels with longitudinal and transversal concrete bridge connectors has not yet been reported in the recent literature. This article assesses the compressive behavior of a sandwich panel with longitudinal ribs. The proposed typology aimed to maintain low self-weight and satisfactory mechanical performance. The influence of longitudinal and transversal concrete bridges on the compressive behavior of the sandwich panels is shown. For this, six specimens with height/thickness ratios of less than 20, with wythes of only 30 mm and a core of 70 mm, were tested under compressive axial loads. In

addition, a comparative study of experimental results and analytical prescriptions predicted from previous analytical models is provided. This analysis aims to evaluate the accuracy of the existing equations to predict the load-carrying capacity of the proposed panels.

3.2 Experimental program

In this study, six specimens of sandwich panels were cast and tested under axial compression. The heights of the tested panels varied from 450 to 2000 mm. Two specimens 2000 mm high were produced with different transversal concrete bridge configurations.

3.2.1 Materials used in the specimens

The tested panels were manufactured with an expanded polystyrene core, while the wythes were made of a waste-based eco-efficient self-compacting microconcrete. The concrete was produced using a High Early Strength Portland Cement (specified in Brazil as CPV type), fine sand, ornamental stone waste, gneiss rock sand and tap water. The mixture was carried out using a 400 L concrete mixer, and to provide high fluidity, a superplasticizer admixture based on polycarboxylates (powerflow 4000, MC Bauchemie) was used.

A 150 mm x 150 mm squared welded steel mesh formed of 4.2 mm steel wires was used to reinforce the wythes. Three 6.3 mm steel rebars and 5.0 mm steel C-type shear connectors were used to reinforce the longitudinal and transversal concrete bridges (ribs). They are placed every 150 mm along the panels' height, connecting the inner and outer wythes (Figure 3.1). Joseph *et al*. (2018) reported premature concrete crushing at load application points due to stress concentration. Because of this, two 10 cm edge beams were cast at the upper and lower ends of the panels to improve the stress distribution and avoid premature failure due to concrete crushing. Expanded polystyrene (EPS) with a thickness of 7 cm was used in the core due to the availability and lowcost. Table 3.1 lists the properties of the steel rebars used in the prototypes.

Table 3.1 – Steel properties.

Application	ϕ (mm)	f_y (MPa)	f_u (MPa)	E_s (GPa)
Concrete bridge reinforcement	5.0	648	728	199
Concrete bridge reinforcement	6.3	541	627	202
Welded mesh	4.2	686	748	195

3.2.2 Design

The prototypes were divided into three groups (Table 3.2). Group A (PA1-PA4) had outer and inner wythes with a thickness of 30 mm and a width of 450 mm, while the thickness of the core was 70 mm. Type C connectors spaced every 150 mm along with the height were used, as shown in Figures 3.1 and 3.2. Group B had an additional transversal 50 mm concrete bridge in the center of the height to reduce the unlocked free length. On the other hand, group C had wythes with a thickness of 35 mm to analyze the influence of increased stiffness in the ultimate load. Therefore, the objective was to compare and validate the panel's behavior with greater overall slenderness.

Table 3.2 – Details and design properties of the proposed specimens.

Group	id	H ×w × t (mm)	H/t	H/b	Core (mm)	Concrete wythe (mm)	f_{ck} (MPa)	E_c (GPa)
A	PA1	2000 x 450 x 130	15.38	4.44	70	30	54	29.4
	PA2	1500 x 450 x 130	11.54	3.33	70	30	37	25.8
	PA3	1000 x 450 x 130	7.69	2.22	70	30	37	25.8
	PA4	400 x 450 x 130	3.08	0.89	70	30	37	25.8
B	PA5	2000 x 450 x 130	15.38	4.44	70	30	54	29.4
C	PA6	2000 x 450 x 140	15.38	4.44	70	35	54	29.4

Figure 3.1- Specimens detailing (left), including reinforced concrete beam (a - Negative reinforcement; b - Positive reinforcement; c -Shear connector).

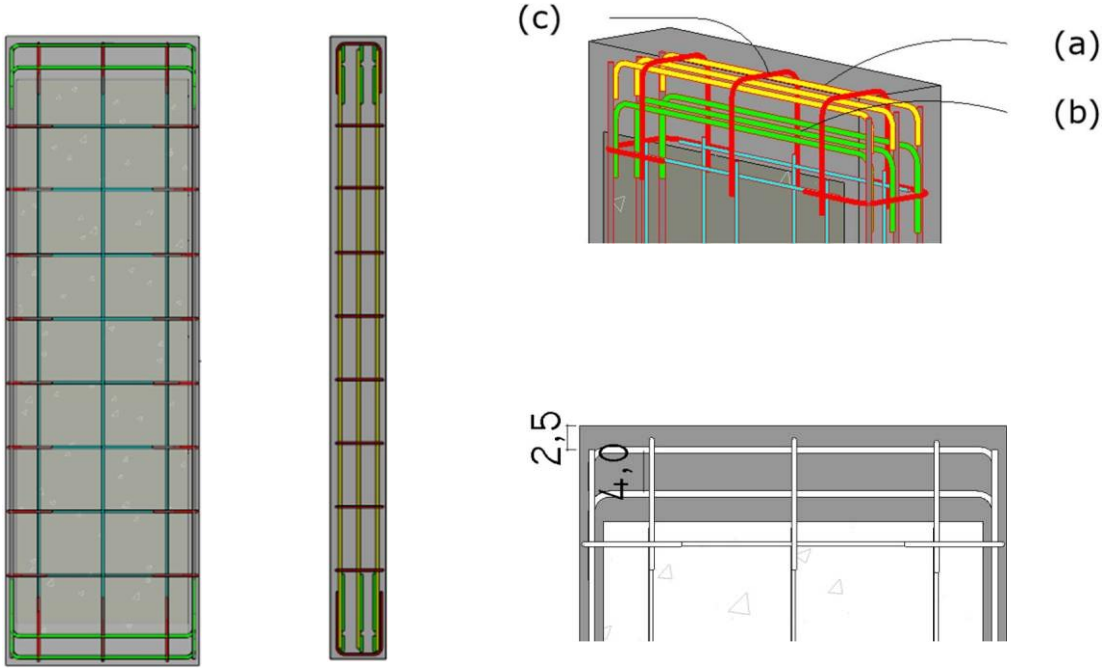

3.2.3 Test procedure

All the prototypes have been cleaned and painted white to observe, read and mark crack patterns easily. The specimens were positioned vertically and centered into the reaction frame. Two 76 mm steel angles were positioned close to the upper edge, acting as a lateral support to prevent lateral displacement. A steel beam was positioned centered on the panel. A 2000 kN hydraulic actuator was used in the tests. A 1000 kN ball joint was used between the beam and the actuator. The measuring dispositive was prepared, checked and adjusted to obtain consistent readings. A pre-load of 50 kN was applied to stabilize the set. Load increments of 50 kN were applied until the appearance of the first cracks, after which the load increment was reduced to 20 kN until the failure. Displacement and strain measurements were recorded using an HBM QuantumX MX840 equipment. In the center of the panel, a 76 mm angle bracket was used to avoid accidents due to sudden fragile failure, following Joseph *et al*. (2018). To avoid early failures due to crushing, in addition to producing a better distribution of loads, 10 cm beams were provided at the top and bottom, as proposed by Serpilli, Clementi and Lenci (2021). Fifteen millimeters plywood plates were used at the bottom and top of the panels to reduce the friction effect between the panel and the metal plate and to avoid stress concentration at load application points, resulting in better distribution of applied load along the panel width. All structural behaviors of the specimens were carefully recorded during the axial compression test (Figure 3.2).

3.2.4 Displacement transducers

Lateral displacement transducers (DT) were positioned at the center of the panel in order to evaluate the stability concerning the height of the prototypes, verifying a possible failure due to buckling. Meanwhile, other transducers were positioned at 1/5 of the height, parallel to the wythe, to capture the localized shortening of the concrete wythes. Above the spreader I-beam, twoDTs were positioned to assess global shortening (Figure 3.3).

Figure 3.2 - Details of the experiment apparatus and assemblage.

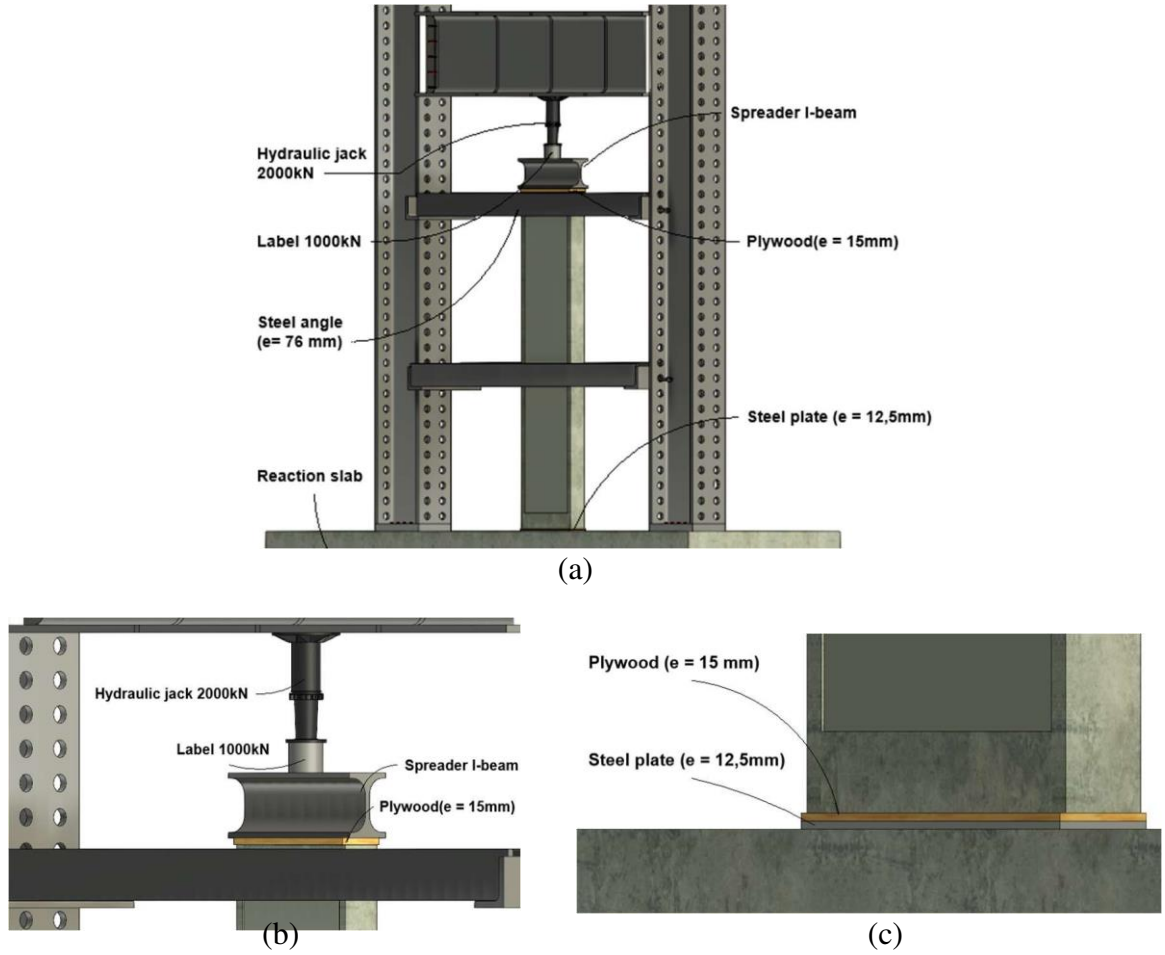

Figure 3.3 - Positioning of the displacement transducers. (a) North side details (b) South side details.

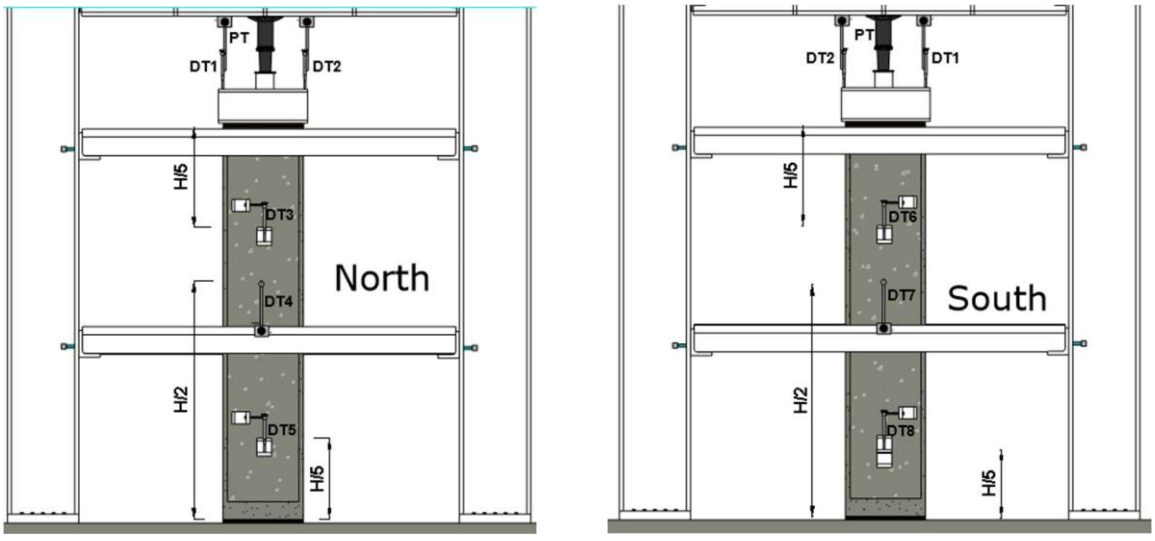

3.2.5 Strain gauges

Two types of electrical strain gauges (SGs) were used. A 6 mm SG, to measure the steel bars strain, and another 70 mm SG, to measure the concrete strain. A total of 12 SGs were used in each sample. Eight SGs of 6 mm were used to measure strain in steel bars and shear connectors, while four SGs of 70 mm were used to measure concrete strain on the wythes of the panel.

3.2.5.1 Steel

To measure the contribution of the steel rebars, four 6 mm SGs were placed on the longitudinalconcrete bridges, with SA1 placed at 1/5 the height from the upper end; SA2 placed at 1/5 the height from the bottom end; SA8 also at 1/5 the height from the bottom end; and SA7 placed at half height, all in the longitudinal direction (Figure 3.4).

Figure 3.4 - Position of electrical strain gauges on longitudinal steel rebars into the lateral concrete bridge.

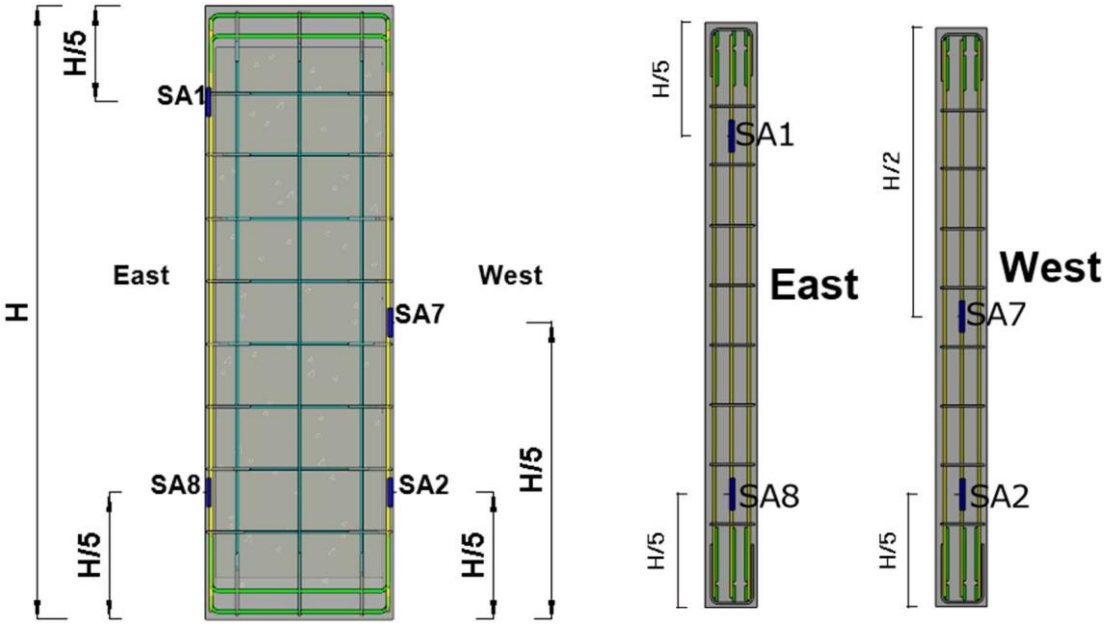

Four 6 mm SGs were placed in the steel grid. SA3 and SA5 were positioned in the center of the panel, with SA3 on the south wythe and SA5 on the north wythe to evaluate deformations in the longitudinal rebars. To measure the transverse strains, the strain gauge SA4 was placed on the south wythe and the SA6 on the north wythe (Figure 3.5).

Figure 3.5 - Position of electrical strain gauges on wythes steel mesh.

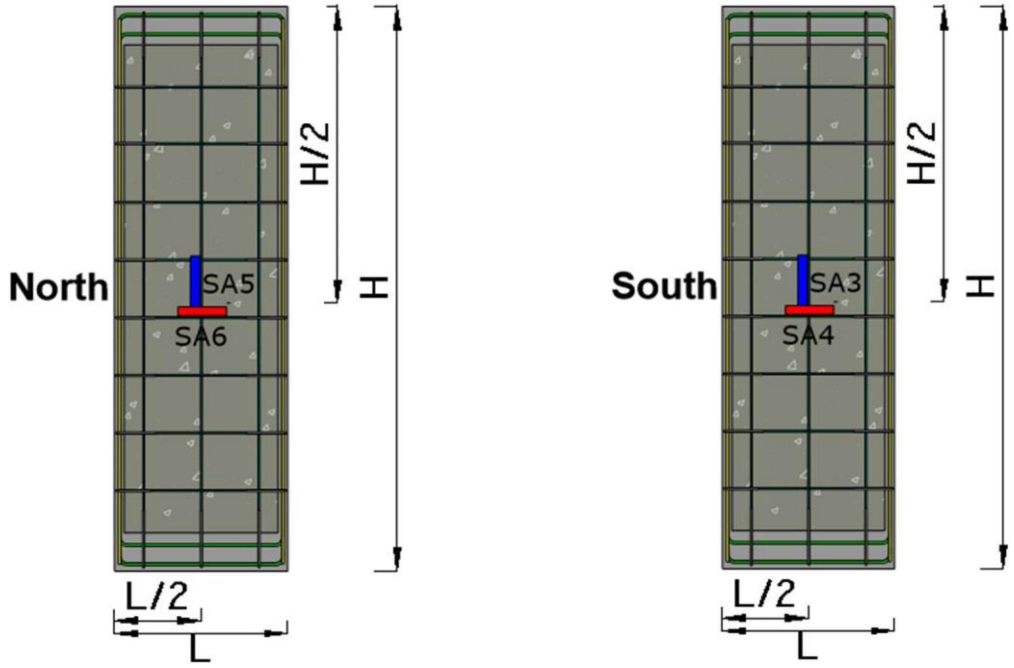

In order to evaluate the effect of the transversal bridges on load-carrying capacity and failure mode, the prototype PA5 was produced. It had an additional 50 mm concrete bridge at its center, with three 6.3 mm bars anchored to the longitudinal concrete bridges at the lateral wythes (Figure3.6). A 6 mm strain gauge (SA9) was installed at its centered rebar.

Figure 3.6 - Position of the electrical strain gauge on the intermediate concrete bridge at the center of the panel.

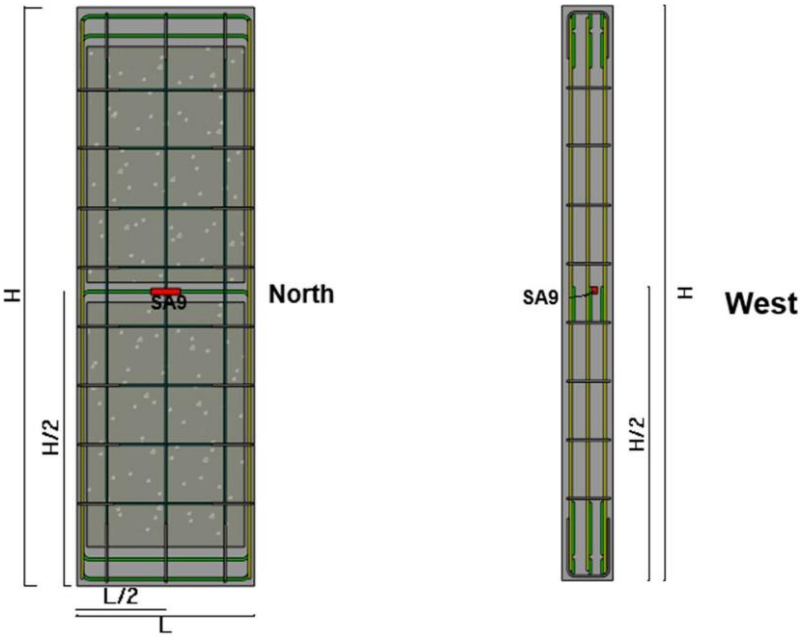

3.2.5.2 Concrete

The 70 mm long SGs were placed on the longitudinal lateral concrete bridges, with SC1 positioned at 1/5 the height from the upper end; and SC4 at 1/5 the height from the bottom end. Meanwhile, to measure the deformations at the center of the prototype, SC2 and SC3 were placed in opposite positions (Figure 3.7).

Figure 3.7 - Position of electrical strain gauges on concrete.

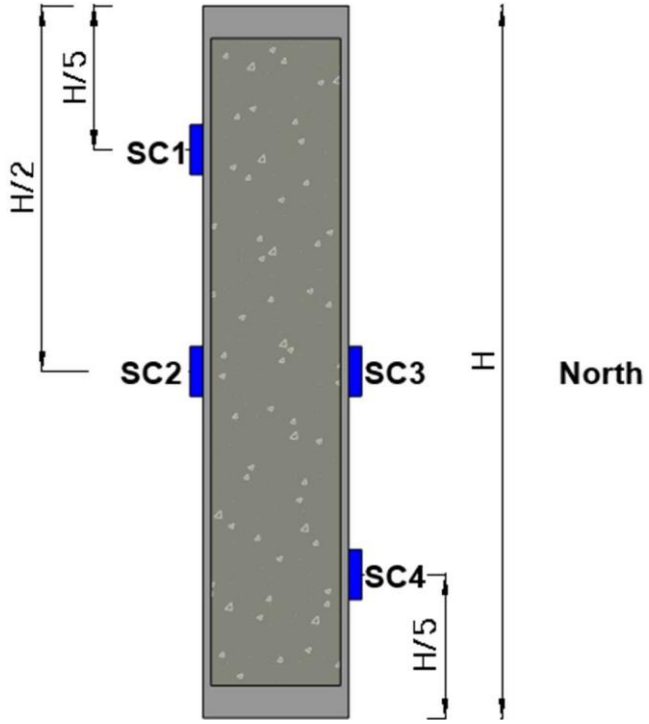

3.3 Structural behavior

The experimental results were analyzed, comprising load-carrying capacity, lateral displacements, vertical displacements, failure modes and cracking patterns.

3.3.1 Cracking pattern and failure modes

The first cracks occurred for loads around 50% of the panels' ultimate capacity, there was a predominance of vertical cracks, and when the rupture was imminent, horizontal cracks began to appear near the upper end (Figure 3.8).

Figure 3.8 - Cracking patterns observed in PA1.

PA3 prototype showed horizontal cracks near the ends and a shear crack for a load of 345 kN near the upper end. This may have occurred due to localized torsion in the connector positioned at that point (Figure 3.13). It had its early failure before reaching 400 kN. The plywood plate at the upper end was not used in this experiment, and stress concentration during the experiment setup occurred. The first cracks took place for 80% of the ultimate load.

Figure 3.9 - Details of the cracks shown in the PA3 prototype.

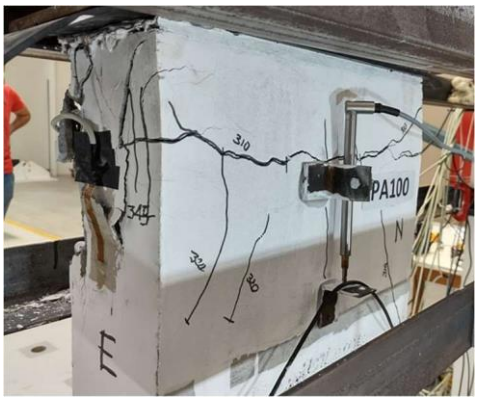

PA6 panel failed due to a possible stress concentration at the bottom end, even with a greater thickness. A possible irregularity in the baseplate may have caused the issue, leading to a

premature rupture. The lack of a cushion able to distribute the loads evenly at the base was solved for the other prototypes with a 15 mm plywood plate (Figure 3.14). The ultimate load reached by the panels was around 350 kN. The panel PA1 with lower concrete wythe thickness reached loads close to 600 kN.

Figure 3.10 - PA5 sandwich panel failure due to stress concentration at the bottom end.

Panel PA4 showed similar failures to PA3, with shear cracks on the east side. Even with low slenderness, the model failed for loads below 400 kN. It presented vertical cracks for about half of its ultimate capacity. For the PA4, the plywood plate was used at both ends, excluding possible stress concentrations due to irregularities in the metal plate (Figure 3.15).

Figure 3.11 - PA4 sandwich panel failure.

3.3.2 Applied load vs. lateral displacement

DTs were installed in 5 full-scale prototypes at half height to evaluate a possible failure due to out-of-plane displacement. Lateral DTs were not used in the specimen with 400 mm height. The results of the measurements are presented in Figure 3.12a. Figure 3.12b shows a comparison between panels PA1 and PA5. The latter had a 50 mm intermediate concrete bridge at half height.

All the prototypes showed brittle failure, so the DTs were removed before the ultimate load. Figure 9a shows a slight out-of-plane displacement for loads up to 400 kN, being a basically linear behavior. The models that showed higher displacements were those with greater slenderness (PA1, PA5 and PA6). Due to the early failure of PA6 by possible stress concentration, obtaining readings for loads above 400 kN was impossible. However, even in models PA1 and PA5, the displacements did not cause loss of stiffness since the main manifestation of rupture was the sudden concrete crushing at the upper or lower ends of panels.

Figure 3.12 – (a) Load vs. displacement curves of the prototypes and (b) comparison between PA5 (with an intermediate transversal concrete bridge) and PA1 (without the intermediate concrete bridge).

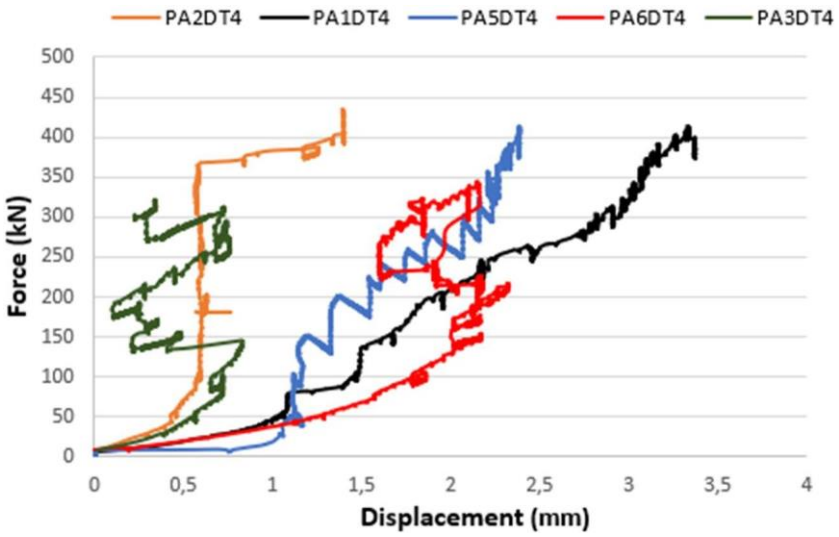

(a)

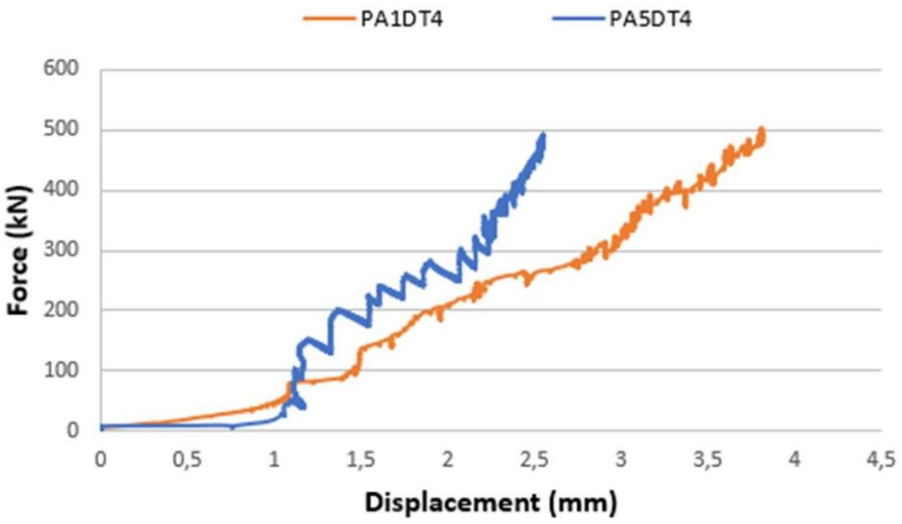

(b)

The graph shows that the PA1 had a displacement 1.5 mm higher than the PA5 for the same load level. Since the analyzed models' failure did not occur by buckling, the concrete bridge did not have a significant contribution. In order to better evaluate the influence of the additional concrete bridge, it would be necessary to produce higher panels, therefore, slenderer, in order to be able to notice the real structural contribution of this component in the ultimate load.

3.3.3 Load vs. strain

The recorded strains can be used to observe points of the highest stresses. Since the prototypes failed mainly by crushing the concrete at the ends, applied load vs. strain analysis was made comparing the prototypes PA1-PA5 (Figure 3.13a) with the steel strain gauges placed at 1/5 the height. Figure 3.13b shows the deformation suffered by the concrete at 1/5 the height from the upper end.

The results shown in Figure 3.13b were practically the same in the different prototypes, considering the same load levels. Regarding the yield stress, the readings were low, considering that the steel yield strain is around 2500 με and the concrete crushing strain of 1800 με. This can occur due to the slipping of the reinforcement bars or even the appearance of localized cracks followed by the crushing of the concrete. Meanwhile, for the strain gauges in the concrete (Figure 3.13b), the deformations were greater, reflecting the failure by crushing the concrete near the upper end.

For panels PA1, PA2 and PA5, the strains close to failure were higher, showing that PA6 and PA3 may have failed due to stress concentration, loss of boundary condition or some accidental eccentricity during the test assembly (Figure 3.13c).

However, even for higher loads, the strain readings by the strain gauges in the steel rebars were still far from the yield strains, showing a possible slip at that point (Figure 3.13d) or even the early failure of the concrete.

The only panel that showed failure at the bottom was PA6 due to a possible stress concentration. Figure 3.10e shows the deformations at 1/5 the height from the bottom end. Comparing the deformations obtained in the other 2000 mm prototypes, this one failed for about half of its capacity.

Figure 3.13 – Load vs. strain curves of the prototypes (a) PA1-PA5 measured by the SA1 strain gauge in the steel rebar at 1/5 height from the upper end; (b) PA1-PA5, measured by the SC1 strain gauge located in the concrete at 1/5 height from the upper end; (c) PA1, PA2 and PA5, measured by the strain gauge SC1 located in the concrete at 1/5 height from the upper end; (d) PA1, PA2 and PA5, measured by the strain gaugeSA1 located in the concrete at 1/5 height of the upper end; (e) PA6, in concrete and steel, measured by SC4 and SA2, respectively, located at 1/5 height from the bottom end; (f) PA1, in the steel, measured by the strain gauge SA3 in the center of the panel connected to the mesh and by the strain gauges SC2 and SC3 located at the center of the longitudinal concrete bridges.

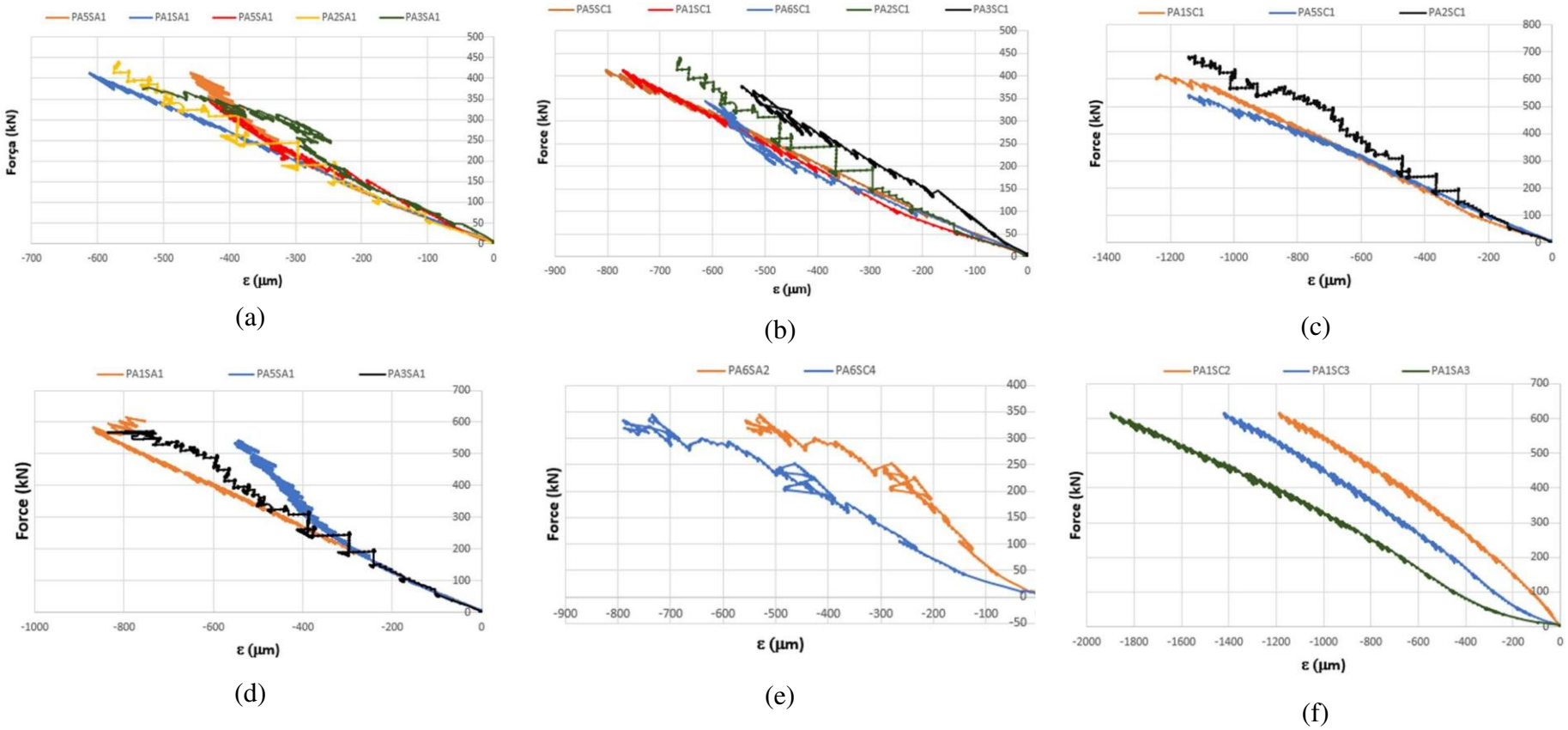

Two concrete strain gauges were positioned at half height, and a steel strain gauge was at the center of the mesh on the panel wythe. Figure 3.10f shows the deformations obtained by the sensors in the PA1 prototype. A possible stress concentration on the panel's west side can be noticed. In addition, the wythes absorbed a greater load compared to the lateral concrete bridges. This can be explained by the thickness of only 30 mm of the concrete layer, implying less stiffness.

3.3.3.1 Load vs. vertical displacement

To evaluate the shortening of the wythes, it was proposed to position transducers at 1/5 the height from the upper and lower ends on both sides of the prototypes. Figure 3.14 evidences the influence of height on the wythe shortening measurements.

The south wythe suffered a greater shortening compared to the north wythe for all the prototypes. Furthermore, by reducing the panel height, a smaller variation was observed. Panel PA1 had a shortening on the south wythe three times greater than the north wythe, while panel PA3 had a virtually equal shortening on both sides.

Figure 3.14 - Wythe shortening measured by the average displacements of the transducers DT3 and DT5 on the north wythe and DT 6 and DT 8 on the south wythe.

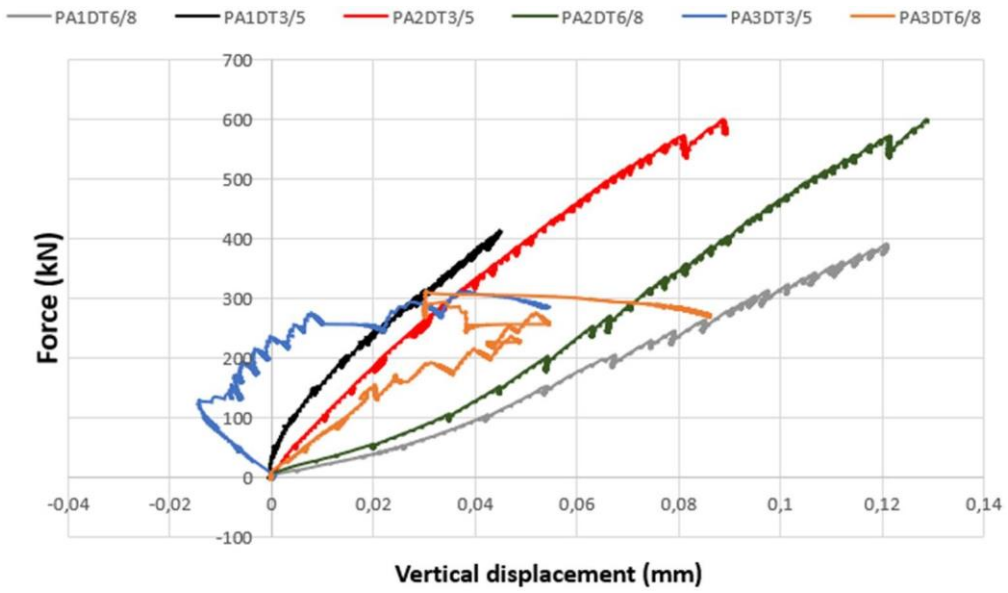

3.4 Prediction equations

The ultimate load-bearing capacity of the panels was compared to results obtained from prediction equations proposed by several authors (Equations 3.1-3.7).

Equation proposed by Leabu (1959).

$$0{,}2f_{cu}A_c\left[1-\left(\frac{H}{40t}\right)^3\right] \qquad \text{Equation 3.1}$$

Equation proposed by Parthasarathy (1977).

$$0{,}57\emptyset f_{cu}A_c\left[1-\left(\frac{kH}{50t}\right)^2\right] \qquad \text{Equation 3.2}$$

Equation proposed by Everard (1977).

$$0{,}55\emptyset f_{cu}A_c\left[1-\left(\frac{kH}{32t}\right)^2\right] \qquad \text{Equation 3.3}$$

Equation proposed by Desayi (1990).

$$0{,}55\emptyset\left[f_{cu}A_c+\left(f_y-f_{cu}\right)A_{sc}\right]\left[1-\left(\frac{kH}{32t}\right)^2\right] \qquad \text{Equation 3.4}$$

Equation proposed by Benayoune *et al*. (2007).

$$0{,}4\emptyset f_{cu}A_c\left[1-\left(\frac{kH}{40t}\right)^2\right]+0{,}67f_yA_s \qquad \text{Equation 3.5}$$

Equation proposed by Mohamad, Omar and Abdullah (2011).

$$0{,}4\emptyset f_{cu}A_c\left[1-\left(\frac{kH}{40(t-\frac{t}{20}}\right)^2\right]+0{,}67f_yA_s \qquad \text{Equation 3.6}$$

Equation proposed by Amran *et al*. (2016).

$$0{,}37\emptyset f_{cu}A_c\left[1-\left(\frac{kH}{32t}\right)^2\right]+0{,}67f_yA_s \qquad \text{Equation 3.7}$$

The equations proposed in 3.1 to 3.7 consider as responsible for the ultimate capacity of the panels the axial compression the ultimate strength of concrete to compression (F_{cu}), the gross area of the panel (A_c), the height of the panel (H), the total thickness of the panel (t), the

boundary condition (k), the yield strength of steel (F_y), the steel area (A_s) and the cracking coefficient of the section (ϕ).

Contrary to the proposed Equations 3.1 to 3.7, Carbonari *et al*. (2013) based their analysis on Euler's hypotheses. The lateral instability failure is verified when the lateral displacement in the center of the panel is equal to half of the displacement necessary to produce buckling in the connectors. To present this mathematically, the author used Equation 3.8, where k_1 and k_2 are the coefficients that represent the boundary condition of the panel, ranging from 0.5 for fixed ends and 1 for pinned ends. The coefficient k_3 (ranging from 0 to 1) takes into account the restriction produced by the EPS and the connectors, while L_C, $\emptyset_c$ and $n_{c,sec}$ represent the length, diameter and number of steel connectors per horizontal line for a certain eccentricity (e). In addition, the buckling height ($L_{buckling}$) is considered according to the boundary condition imposed at the ends of the panel, while E_m and I_{layer} represent the modulus of elasticity of the concrete and the moment of inertia of the layer section. With that, Carbonari *et al*. (2013) managed to ignore the influence of EPS on material inertia and, therefore, proposed an equation with more details.

$$P_{max} = \frac{8E_m I_{layer}}{{k_2}^2 {L_{buckling}}^2}\left[acos\left(\frac{1}{1+\frac{n_{c,sec}\pi^2 {\emptyset_c}^2}{32ek_3{k_1}^2 L_c}}\right)\right]^2 \qquad \text{Equation 3.8}$$

In order to compare the ultimate loads predicted by the equations with the experimental results, graphs were plotted with the data shown in Table 3.3 using the four slenderness variations of this study.

Table 3.3 – Ultimate load predicted using equations proposed by different authors for thepanels evaluated in this study.

Authors	**P_u (kN) PA1**	**P_u (kN) PA2**	**P_u (kN) PA3**	**P_u (kN) PA4**
Leabu (1959)	408.3	621.9	629.5	631.6
Pillai (1977)	843. 2	1235.7	1241.4	1256.8
ACI (1977)	785.2	1158.0	1171.2	1207.6
Saheb (1989)	895.7	1238.4	1243.4	1263.1
Benayoune et al. (2007)	804.1	1022.2	1009.8	989.6
Mohamad, Omar and Abdullah (2011)	1050.8	1385.5	1376.7	1375.6
Carbonari et al. (2013)	636.0	716.8	395.7	393.6
Amran et al. (2016)	975.1	1277.7	1271.8	1306.8
Experimental	621.8	707.3	377.5	383.2

The graph in Figure 3.15 shows the results obtained by the equations compared to the experimental results. To relate the equations with the results obtained, *k* was considered equal to 0.5 and 0.7 for panels PA1 and PA2. However, the only equation that managed to get as closeto the experimental results was that of Carbonari *et al*. (2013) because, in addition to the boundary condition (*k*), they consider an accidental eccentricity during the test and disconsider the EPS in the ultimate capacity of the prototypes.

Figure 3.15 - Comparison of the experimental results with predictions obtained from equations proposed by different authors.

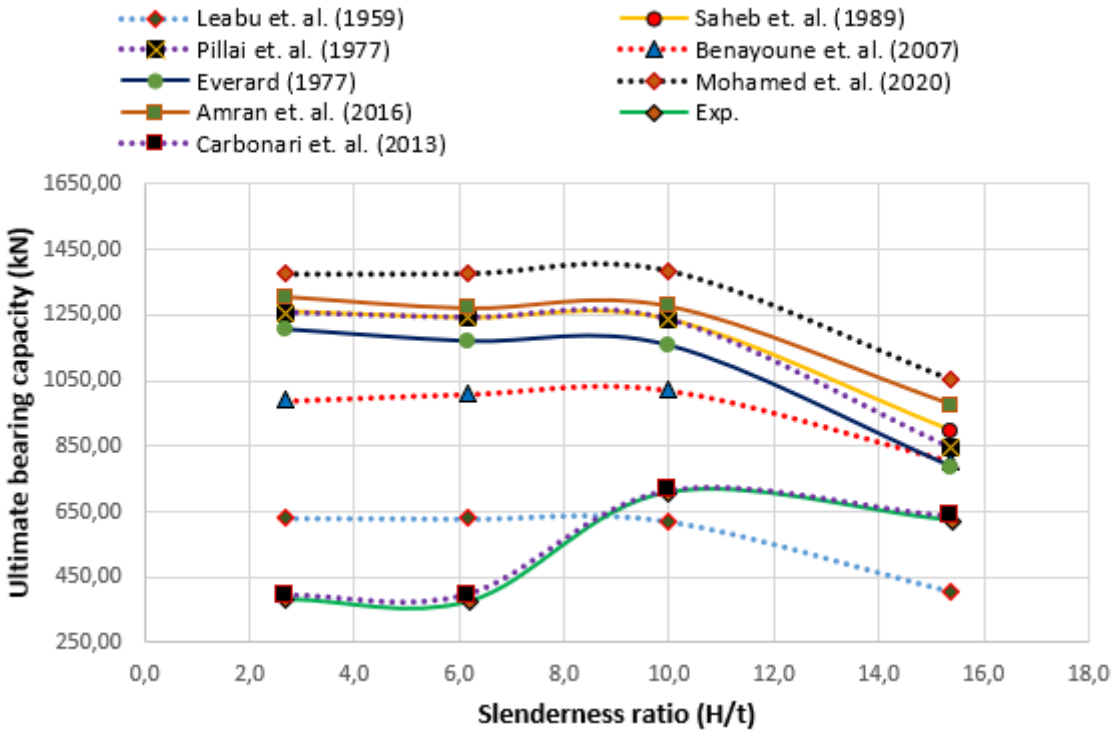

Due to the unintentional disturbances during the experimental apparatus assembly and testing, which can produce accidental eccentricity and affect the maintenance of the boundary condition and the maximum load reached by the prototype, the equation proposed by Carbonari *et al*. (2013) was used in an attempt to assess possible influences since it considers the eccentricity parameter (Table 3.4).

The results suggest a possible boundary condition failure for the prototypes PA1 and PA2. These reached loads greater than 600 kN, causing the expulsion of the angle that restricted its upper end and a loss of the boundary condition and possible early failure. For PA3 and PA4, its believed the boundary condition was preserved due to the reduced loads, but an accidental eccentricity imposed during the test may have caused an early failure (Figure 3.11).

Table 3.4 - Ultimate capacity obtained using the equation proposed by Carbonari *et al*. (2013),varying the parameters of eccentricity and boundary condition.

Panel	E_m	I_{layer}	k_2	$L_{buckling}$	$n_{c,sec}$	$\square_c$	e	k_3	k_1	L_c	P_{max}
PA1	2583	202.5	0.5	200	28	0.5	0.1	0.5	0.5	40	636.0
PA2	2940	202.5	0.7	130	18	0.5	0.1	0.8	0.75	40	716.8
PA3	2940	202.5	1	80	12	0.5	0.3	1	1	40	395.7
PA4	2940	202.5	1	35	4	0.5	3	1	1	40	393.6

3.5 Conclusions

This article evaluated the mechanical performance of 6 models of a new sandwich panel typology using C-type connectors and longitudinal concrete bridges to connect the two concrete wythes at axial compression. An analysis of the influence of the variation of the global slenderness between 4 and 16 on the parameters of deformations, displacements, failure modes and ultimate capacity of the prototypes was made. The main conclusions are listed as follows:

- The predominant failure mode was crushing the concrete at the upper or bottom ends ofthe panels.
- The first cracks occurred for loads between 50% and 80% of the measured ultimate capacity.

- The longitudinal concrete bridges contributed to the stability since the detachment of the wythes in relation to the EPS core was not observed. On the other hand, the strains were low considering the plastification strain of ordinary concrete of 2000 με and 10000 με for steel.
- Prototypes PA1 and PA2 reached loads above 600 kN. For them, the loss of the initial boundary condition was evidenced by the expulsion of the upper angle, leading to an early failure.
- Prototypes PA3 and PA4 failed for loads below 400 kN, suggesting the occurrence of some eccentricity in the positioning of the beam responsible for transferring the load to the panel.
- The ultimate loads measured were compared to results obtained using prediction equations proposed by different authors. The equation proposed by Carbonari *et al*. (2013) better fit the experimental results, effectively predicting the early failure caused by accidental eccentricity or loss of boundary conditions.

More studies are required for a more in-depth understanding of the structural behavior of this panel typology, expanding the experimental program to include flexural, flexo-compression, and eccentric axial compression tests. Calibrating numerical models for non-linear analysis able to reproduce the experimental results is also of great interest.

CHAPTER 4. General conclusion

4.1 General conclusions

This dissertation presented detailed information about the performance of sandwich panels under axial compression. In addition, a new typology was proposed, and its ability to be used as a structural element was evaluated in the laboratory.

Due to the lack of regulations, applying this constructive model becomes even more complex. However, sandwich panels stand out with their lightness and structural capacity when it comes to precast since transport is of paramount importance for the precast industry, as the heavier the parts, the greater the transport costs. In this context, sandwich walls with their low-density core stand out among other types of panels.

However, due to industrialization in civil construction, the implementation costs are still high when compared to traditional methods, and part of this differentiation is the use of specialized equipment and labor; however, this construction method is considered a significant advance in the civil construction industry and has been gaining ground.

4.2 Proposals for future works

The research focused on sandwich panels has a wide area of analysis. Due to the various applications and the possibility of diversification in geometry, this constructive element can be used as floors, facade panels, and load-bearing panels in addition to its application in the aerospace and naval industry, which already has wide application. Due to the lack of regulations, the experimental analysis of sandwich panels is of academic importance. Among the extensive studies, the following analyzes can be proposed:

- Numerical analysis of the proposed models makes it possible to describe with greater precision the structural behavior for possible applications.
- Analyze the bending since wind stress becomes significant when applied to the facades of large buildings and can cause the panels' failure.
- Acoustic and thermal evaluations since the sandwich panels constituted of the low-density core can be used as an acoustic and thermal insulator.
- Analyze the influence of other types of shear connectors on composite behavior.
- Propose alternative materials such as carbon fiber and fiberglass that can reduce cement consumption, as this is a major cause of the low eco-efficiency of precast products. This would bring sustainability to the production and application of these structures.

REFERENCES

AAMIR MAZHAR, M. *et al.* An experimental investigation of thermocol impregnated ferrocement panel as an alternate building material. **Materials Today: Proceedings**, [*s. l.*], 2021.

ABBADI, A. *et al.* Static and fatigue characterization of sandwich panels. **Materials Science Forum**, [*s. l.*], v. 518, p. 555–562, 2006.

AHMAD, A.; SINGH, Y. In-plane behaviour of expanded polystyrene core reinforced concretesandwich panels. **Construction and Building Materials**, [*s. l.*], v. 269, p. 121804, 2021a.

AHMED, S.; ALI, M. Use of agriculture waste as short discrete fibers and glass-fiber-reinforced-polymer rebars in concrete walls for enhancing impact resistance. **Journal of Cleaner Production**, [*s. l.*], v. 268, p. 122211, 2020.

AHN, B. Y. *et al.* Printed origami structures. **Advanced Materials**, [*s. l.*], v. 22, n. 20, p. 2251–2254, 2010.

AKTAY, L.; JOHNSON, A. F.; KRÖPLIN, B. H. Numerical modelling of honeycomb corecrush behaviour. **Engineering Fracture Mechanics**, [*s. l.*], v. 75, n. 9, p. 2616–2630, 2008.

ALCHAAR, A.; ABED, F. Finite element analysis of a thin-shell concrete sandwich panel under eccentric loading. **Journal of Building Engineering**, [*s. l.*], v. 32, n. January, p. 101804, 2020.

ATOYEBI OLUMOYEWA, D. *et al.* Splitting tensile strength assessment of lightweight foamed concrete reinforced with waste tyre steel fibres. **International Journal of CivilEngineering and Technology**, [*s. l.*], v. 9, n. 9, p. 1129–1137, 2018.

BAI, F.; DAVIDSON, J. S. Analysis of partially composite foam insulated concrete sandwichstructures. **Engineering Structures**, [*s. l.*], v. 91, p. 197–209, 2015.

BENAYOUNE, A. *et al.* Response of pre-cast reinforced composite sandwich panels to axial loading. **Construction and Building Materials**, [*s. l.*], v. 21, n. 3, p. 677–685, 2007.

CARBONARI, G. *et al.* Estudio experimental y analítico sobre el comportamiento a compresión de paneles sandwich con eps. **Materiales de Construccion**, [*s. l.*], v. 63, n. 311, p.393–402, 2013.

CHEN, A. *et al.* Experimental investigation and finite element analysis of flexural behavior of insulated concrete sandwich panels with FRP plate shear connectors. **Engineering Structures**,[*s. l.*], v. 98, p. 95–108, 2015.

CHOI, I.; KIM, J. H.; KIM, H. R. Composite behavior of insulated concrete sandwich wall panels subjected to wind pressure and suction. **Materials**, [*s. l.*], v. 8, n. 3, p. 1264–1282, 2015.

CODYRE, L.; FAM, A. The effect of foam core density at various slenderness ratios on axial strength of sandwich panels with glass-FRP skins. **Composites Part B: Engineering**, [*s. l.*], v. 106, p. 129–138, 2016. Disponível em: http://dx.doi.org/10.1016/j.compositesb.2016.09.016.

CORE, S. Best Practice Guide for Sandwich Structures in Marine Applications. **Best PracticeGuide for Sandwich Structures in Marine Applications**, [*s. l.*], p. 279, 2013.

CUI, Y. *et al.* Failure mechanism of geopolymer composite lightweight sandwich panel under flexural and edgewise compressive loads. **Construction and Building Materials**, [*s. l.*], v. 270,p. 121496, 2021. Disponível em: https://doi.org/10.1016/j.conbuildmat.2020.121496.

DANIEL RONALD JOSEPH, J.; PRABAKAR, J.; ALAGUSUNDARAMOORTHY, P.
Flexural behavior of precast concrete sandwich panels under different loading conditions suchas punching and bending. **Alexandria Engineering Journal**, [*s. l.*], v. 57, n. 1, p. 309–320, 2018.

DASKIRAN, E. G.; DASKIRAN, M. M.; GENCOGLU, M. Development of fine-grained

concretes for textile reinforced cementitious composites. **Computers and Concrete**, [*s. l.*], v. 18, n. 2, p. 279–295, 2016.

DAVID C. SALMON, and A. E. P ARTIALLY COMPOSITE SANDWICH PANEL DEFLECTIONS. **Journal of Structural Engineering**, [*s. l.*], v. 121, n. 4, p. 778–783, 1995.

DAWOOD, M. *et al.* Static and fatigue bending behavior of pultruded GFRP sandwich panelswith through-Thickness fiber insertions. **Composites Part B: Engineering**, [*s. l.*], v. 41, n. 5, p. 363–374, 2010. Disponível em: http://dx.doi.org/10.1016/j.compositesb.2010.02.006.

DESAYI, S. M. S. A. P. ULTIMATE STRENGTH OF R.C. WALL PANELS IN Two-WAY IN-PLANE ACTION By S. Madina Saheb 1 and Prakash Desayi 2. [*s. l.*], v. 116, n. 5, p. 1384–1402, 1990.

DUTRA, J. R. *et al.* Investigations on sustainable honeycomb sandwich panels containing eucalyptus sawdust, Piassava and cement particles. **Thin-Walled Structures**, [*s. l.*], v. 143, n.October 2018, p. 106191, 2019.

EVERARD, G. D. O. and N. J. Investigation of Reinforced Concrete Walls. **ACI Journal Proceedings**, [*s. l.*], v. 74, n. 6, 1977.

FISHER, D. Title: Rotating Tower Dubai Rotating Tower Dubai. **Ctbuh Resaerch Paper**, [*s. l.*], 2008.

FLANSBJER, M. *et al.* Composite Behaviour of Textile Reinforced Reactive Powder ConcreteSandwich Façade Elements. **International Journal of Concrete Structures and Materials**, [*s. l.*], v. 12, n. 1, p. 71, 2018.

FRANKL, B. A. *et al.* Behavior of precast, prestressed concrete sandwich wall panels reinforced with CFRP shear grid. **PCI Journal**, [*s. l.*], v. 56, n. 2, p. 42–54, 2011.

FRAZÃO, C. *et al.* Development of sandwich panels combining Sisal Fiber-Cement Composites and Fiber-Reinforced Lightweight Concrete. **Cement and Concrete Composites**,[*s. l.*], v. 86, p. 206–223, 2018.

GARA, F. *et al.* Experimental tests and numerical modelling of wall sandwich panels.

Engineering Structures, [*s. l.*], v. 37, p. 193–204, 2012.

GAY, D.; HOA, S. V. **Composite Materials : Design and Applications, Second Edition**. [*S.l.: s. n.*], 2007. Disponível em: https://www.taylorfrancis.com/books/mono/10.1201/9781420045208/composite-materials- daniel-gay-suong-hoa.

GRAZIANI, L. *et al.* A more sustainableway for producing RC sandwich panels on-site and indeveloping countries. **Sustainability (Switzerland)**, [*s. l.*], v. 9, n. 3, 2017.

HASSAN, T. K.; RIZKALLA, S. H. 2010 - Hassan e Rizkalla. [*s. l.*], p. 147–162, 2010.

HOPKINS, P. M.; NORRIS, T.; CHEN, A. Creep behavior of insulated concrete sandwich panels with fiber-reinforced polymer shear connectors. **Composite Structures**, [*s. l.*], v. 172, p. 137–146, 2017. Disponível em: http://dx.doi.org/10.1016/j.compstruct.2017.03.038.

KIM, J. H.; YOU, Y. C. Composite behavior of a novel insulated concrete sandwich wall panelreinforced with GFRP shear grids: Effects of insulation types. **Materials**, [*s. l.*], v. 8, n. 3, p. 899–913, 2015.

KUJALA, P.; KLANAC, A. STEEL SANDWICH PANELS IN MARINE APPLICATIONS Pentti KUJALA Alan KLANAC Steel Sandwich Panels in Marine Applications. [*s. l.*], v. 56, p. 305–314, 2005.

LAMEIRAS, R. *et al.* Development of sandwich panels combining fibre reinforced concrete layers and fibre reinforced polymer connectors. Part I: Conception and pull-out tests. **Composite Structures**, [*s. l.*], v. 105, p. 446–459, 2013. Disponível em: http://dx.doi.org/10.1016/j.compstruct.2013.06.022.

LEABU, V. F. Problems and Performance of Precast Concrete Wall Panels. **ACI Journal Proceedings**, [*s. l.*], v. 56, n. 10, 1959.

LEE, J. H. *et al.* Structural Behavior of Durable Composite Sandwich Panels with High Performance Expanded Polystyrene Concrete. **International Journal of Concrete**

Structuresand Materials, [*s. l.*], v. 12, n. 1, 2018.

MAMALIS, A. G. *et al.* Experimental investigation of the collapse modes and the main crushing characteristics of composite sandwich panels subjected to flexural loading. **International Journal of Crashworthiness**, [*s. l.*], v. 13, n. 4, p. 349–362, 2008.

MOHAMAD, N.; OMAR, W.; ABDULLAH, R. Precast Lightweight Foamed Concrete Sandwich Panel (PLFP) tested under axial load: Preliminary results. **Advanced Materials Research**, [*s. l.*], v. 250–253, p. 1153–1162, 2011.

MUGAHED AMRAN, Y. H. *et al.* Design innovation, efficiency and applications of structuralinsulated panels: A review. **Structures**, [*s. l.*], v. 27, n. July, p. 1358–1379, 2020.

MUGAHED AMRAN, Y. H. *et al.* Influence of slenderness ratio on the structural performanceof lightweight foam concrete composite panel. **Case Studies in Construction Materials**, [*s. l.*], v. 10, p. 1–24, 2019.

MUGAHED AMRAN, Y.H. *et al.* Structural behavior of axially loaded precast foamed concrete sandwich panels. **Construction and Building Materials**, [*s. l.*], v. 107, p. 307–320, 2016.

NEVEU, F.; CASTANIÉ, B.; OLIVIER, P. The GAP methodology: A new way to design composite structures. **Materials and Design**, [*s. l.*], v. 172, p. 107755, 2019. Disponível em: https://doi.org/10.1016/j.matdes.2019.107755.

NOURI DAMGHANI, M.; MOHAMMADZADEH GONABADI, A. Investigation of Energy Absorption in Aluminum Foam Sandwich Panels By Drop Hammer Test: Experimental Results. **Mechanics, Materials Science & Engineering**, [*s. l.*], v. 7, n. December, p. 123–141, 2016. Disponível em: http://mmse.xyz/en/investigation-of-energy-absorption-in-aluminum-foam-sandwich-panels-by-drop-hammer-test-experimental-results/.

O'HEGARTY, R.; KINNANE, O. Review of precast concrete sandwich panels and their innovations. **Construction and Building Materials**, [*s. l.*], v. 233, p. 117145, 2020. Disponível em: https://doi.org/10.1016/j.conbuildmat.2019.117145.

O'HEGARTY, R. *et al.* Composite behaviour of fibre-reinforced concrete sandwich panels

withFRP shear connectors. **Engineering Structures**, [*s. l.*], v. 198, n. June, p. 109475, 2019. Disponível em: https://doi.org/10.1016/j.engstruct.2019.109475.

PANJEHPOUR, M.; ALI, A. A. A.; VOO, Y. L. Structural Insulated Panels: Past, Present, andFuture. **Journal of Engineering, Project, and Production Management**, [*s. l.*], v. 3, n. 1, p. 2–8, 2013.

PARTHASARATHY, S. U. P. C. V. Ultimate Strength and Design of Concrete i i o /. **Buildingand Environment**, [*s. l.*], v. 12, p. 25–29, 1977.

PEČUR, I. B. *et al.* Precast Sandwich Panel – Innovative Way of Construction. **10th CCCCongress LIBEREC**, [*s. l.*], n. October, p. 1–12, 2014.

PESSIKI, S.; MLYNARCZYK, A. **Experimental Evaluation of the precast concrete walls**.[*S. l.: s. n.*], 2003.

QIN, Y. *et al.* Truss spacing on innovative composite walls under compression. **Journal of Constructional Steel Research**, [*s. l.*], v. 160, p. 1–15, 2019. Disponível em: https://doi.org/10.1016/j.jcsr.2019.05.027.

QUN, X.; SHUAI, W.; CHUN, L. Axial Compression Behavior of a New Type of PrefabricatedConcrete Sandwich Wall Panel. **IOP Conference Series: Materials Science and Engineering**,[*s. l.*], v. 317, p. 012063, 2018.

RATHBUN, H. J. *et al.* Performance of metallic honeycomb-core sandwich beams under shockloading. **International Journal of Solids and Structures**, [*s. l.*], v. 43, n. 6, p. 1746–1763, 2006.

REJAB, M. R. M.; CANTWELL, W. J. The mechanical behaviour of corrugated-core sandwichpanels. **Composites Part B: Engineering**, [*s. l.*], v. 47, p. 267–277, 2013.

SEEBER, K. E. *et al.* State-of-the-art of precast/prestressed sandwich wall panels. **PCI Journal**, [*s. l.*], v. 42, n. 2, p. 92–134, 1997.

SERPILLI, M.; CLEMENTI, F.; LENCI, S. An experimental and numerical study on the in-

plane axial and shear behavior of sprayed in-situ concrete sandwich panels. **Engineering Structures**, [*s. l.*], v. 232, n. April 2021, p. 111814, 2021. Disponível em: https://doi.org/10.1016/j.engstruct.2020.111814.

SHAMS, A.; HORSTMANN, M.; HEGGER, J. Experimental investigations on textile-reinforced concrete (TRC) sandwich sections. **Composite Structures**, [*s. l.*], v. 118, n. 1, p. 643–653, 2014.

SMITH, R. E. **Prefab Architecture: A Guide to Modular Design and Construction**. [*S. l.: s. n.*], 2011-. ISSN 1098-6596. Disponível em: http://books.google.com/books?hl=en&lr=&id=pOCliGMKpzUC&oi=fnd&pg=PT20&dq=PREFAB+ARCHITECTURE:+a+guide+to+modular+design+and+construction&ots=j0n5GteYZ6&sig=wUYE0qhNDvy5tN_r6P9WQe79p4U.

TOMBLIN, J. *et al.* Review of Damage Tolerance for Composite Sandwich Airframe Structures. **~Bericht**, [*s. l.*], p. 71, 1999. Disponível em: www.tc.faa.gov/its/act141/reportpage.html in.

TOMLINSON, D.; FAM, A. Axial load-bending moment-interaction diagram of partially composite precast concrete sandwich panels. **ACI Structural Journal**, [*s. l.*], v. 115, n. 6, p. 1515–1528, 2018.

VALENTE, I.; CRUZ, P. J. S. Experimental analysis of Perfobond shear connection between steel and lightweight concrete. **Journal of Constructional Steel Research**, [*s. l.*], v. 60, n. 3–5, p. 465–479, 2004.

VINSON, J. R. Sandwich Structures: Past, Present, and Future. **Sandwich Structures 7: Advancing with Sandwich Structures and Materials**, [*s. l.*], p. 3–12, 2005.

YAN, L. L. *et al.* Compressive strength and energy absorption of sandwich panels with aluminum foam-filled corrugated cores. **Composites Science and Technology**, [*s. l.*], v. 86, p.142–148, 2013.

YANG, X. *et al.* Crashworthiness investigation of the bio-inspired bi-directionally corrugated core sandwich panel under quasi-static crushing load. **Materials and Design**, [*s.*

l.], v. 135, p.275–290, 2017. Disponível em: http://dx.doi.org/10.1016/j.matdes.2017.09.040.

YAZDANI SARVESTANI, H. *et al.* 3D printed architected polymeric sandwich panels: Energy absorption and structural performance. **Composite Structures**, [*s. l.*], v. 200, n. April,p. 886–909, 2018.

YAZDANI SARVESTANI, H. *et al.* 3D printed architected polymeric sandwich panels: Energy absorption and structural performance. **Composite Structures**, [*s. l.*], v. 200, n. April,p. 886–909, 2018b. Disponível em: https://doi.org/10.1016/j.compstruct.2018.04.002.

ZHOU, J.; GUAN, Z. W.; CANTWELL, W. J. Scaling effects in the mechanical response of sandwich structures based on corrugated composite cores. **Composites Part B: Engineering**, [*s. l.*], v. 93, p. 88–96, 2016.